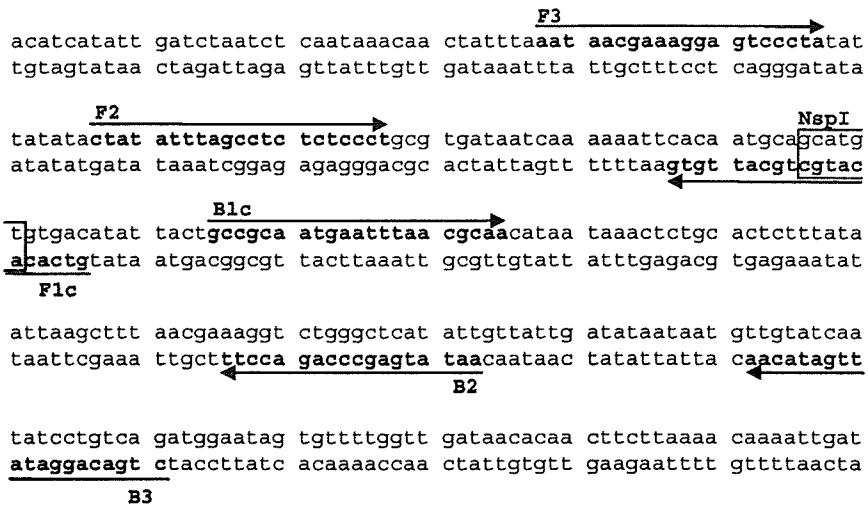

(B)

Primer	Sequence (5'-3')
F3	AATAACGAAAGGAGTCCCTA
B3	CTGACAGGATATTGATACAACA
FIP (F1c + T_4 + F2)	GTCACACATGCTGCATTGTGTTTTCTATATTTAGCCTCTCTCCCT
BIP (B1c+ T_4 + B2)	GCCGCAATGAATTTAACGCAATTTTAATATGAGCCCAGACCTT

Fig. 1. Primer design for RT-LAMP for the detection of ZEBOV. (A) Sequence data of the partial trailer region from position 18,301–18,610 (ZEBOV strain Mayinga, GenBank Accession no. AF086833). The arrows show the location of the primer binding sequence and the direction of primer extension. *Nsp*I restriction sites are boxed. (B) Sequences of primers used for RT-LAMP.

30 min at 37 °C with 0.2 μg of the linearized plasmid. Two units of RQ1 RNase-free DNase (Promega) were then added and incubation was continued for a further 15 min. The reactions were incubated for 15 min at 70 °C to inactivate the DNase. The transcripts were extracted using an RNeasy mini kit (Qiagen, Hilden, Germany), and resuspended in 50 μL of DEPC-treated water. The concentration of RNA transcript was determined by measuring the optical density (OD) at 260 nm.

2.5. RT-LAMP assay

The RT-LAMP reaction was performed with a Loopamp RNA amplification kit (Eiken Chemical Co. Ltd., Tokyo, Japan) in accordance with the manufacturer's protocol. A 25-μL reaction mixture containing 40 pmol each of primers FIP and BIP, 5 pmol each of the outer primers F3 and B3, 12.5 μL of 2× reaction mix, 1.0 μL of amplification mixture containing *Bst* DNA polymerase and avian myeloblastosis virus reverse transcriptase, and 2.0 μL of RNA sample was incubated at 63 °C for 60 min and then heated at 80 °C for 2 min to terminate the reaction in a thermal cycler (Mastercycler; Eppendorf, Hamburg, Germany). A portion of each amplified product was analyzed on a 3% agarose gel, followed by staining with ethidium bromide and visualization on an imaging analyzer (LAS-3000; FujiFilm, Tokyo, Japan). For real-time monitoring of amplification by RT-LAMP assay, the reaction mixtures were incubated at 63 °C and observed by spectrophotometric analysis using a real-time turbidimeter (LA-200; Teramecs, Kyoto, Japan). The time of positivity observed through real time RT-LAMP assay was determined as the time at which the turbidity reached the threshold value fixed at 0.1, which is double the average turbidity value of negative controls of several replicates. The specificity of the RT-LAMP-amplified products was validated with a restriction enzyme digestion (Notomi et al., 2000). The extracted RT-LAMP products were digested with *Nsp*I at 37 °C overnight and analyzed by 3% agarose gel electrophoresis.

3. Results

3.1. Evaluation of RT-LAMP for EBOV using the artificial RNA transcribed in vitro

For specific amplification of the genomic RNA of ZEBOV, we designed a set of four oligonucleotide primers comprising two inner (FIP, BIP) and two outer primers (F3, B3) with six recognition sites (Fig. 1A and B). The six sites within the trailer region, which are highly conserved among ZEBOV strains, were selected as targets for primer binding.

In the initial examination, in vitro transcribed ZEBOV RNA which encodes antisense GFP with the ZEBOV trailer or leader sequence at either end was used to evaluate the RT-LAMP assay. A successful RT-LAMP reaction with virus-specific primers produced the characteristic ladder-like pattern on agarose gel electrophoresis (Fig. 2A). To confirm that the products were amplified from the target region, the products were digested with *Nsp*I. *Nsp*I digestion produced fragments of 136 and 69 bp as predicted from the expected DNA structures, indicating that the reaction was specific (Fig. 2A).

The sensitivity of the RT-LAMP assay for ZEBOV was determined by testing serial 10-fold dilutions of artificial ZEBOV

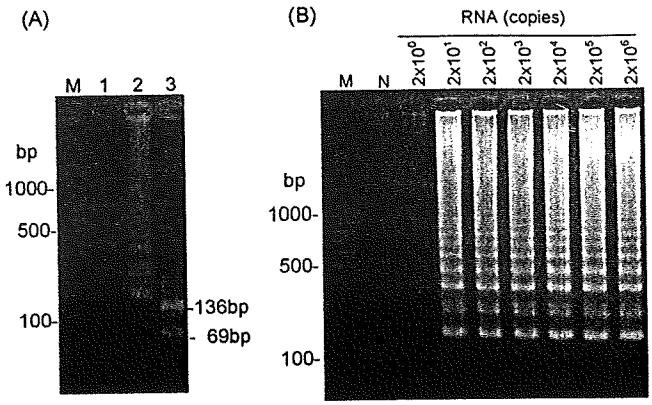

Fig. 2. RT-LAMP assay using in vitro transcribed ZEBOV RNA. (A) Electrophoretic analysis of RT-LAMP products on 3% agarose gel. RT-LAMP was carried out at 63 °C for 60 min. Amplification showed a ladder-like pattern. Lane 1, RT-LAMP with distilled water (negative control); Lane 2, RT-LAMP with in vitro transcribed ZEBOV RNA; Lane 3, RT-LAMP products from Lane 2 after digestion with *NspI*; M, 100-bp DNA ladder. (B) Sensitivity of RT-LAMP using 10-fold serial dilutions of in vitro transcribed ZEBOV RNA. RT-LAMP was carried out at 63 °C for 60 min. N, negative control; M, 100-bp DNA ladder.

RNA. As shown in Fig. 2B, the assay could detect more than 20 copies of the artificial RNA in the reaction at 63 °C for 60 min. To examine the real-time amplification, the reactions at different concentrations of RNA ranging from 2 to 2×10^6 copies were monitored by measuring the turbidity in real-time. The threshold value was fixed at turbidity of 0.1, and samples with turbidity above this threshold value were considered positive. The times of positivity observed through real-time monitoring were found to be 16 or 26 min at a concentration of 2×10^6 or 20 copies, respectively (Fig. 3).

3.2. *Specificity and sensitivity of RT-LAMP for intact viral RNA*

To evaluate the specificity of the RT-LAMP assay for ZEBOV, intact viral RNAs from cell-culture derived viral stocks of two ZEBOV strains, two SEBOV strains, one ICEBOV strain, and four MARV strains, were subjected to RT-LAMP assay. Viral RNAs were extracted from each virus stock and RNAs equivalent to 10^4 FFU were tested in the RT-LAMP assay. As shown

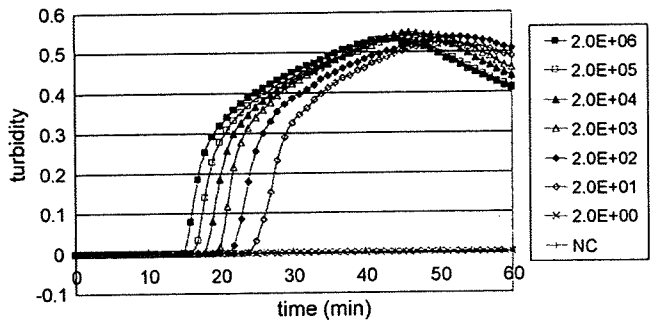

Fig. 3. Kinetics of RT-LAMP reaction for in vitro transcribed ZEBOV RNA. RT-LAMP was performed at 63 °C for 60 min. Serial 10-fold dilutions of in vitro transcribed RNA were subjected to RT-LAMP and monitored by measurement of turbidity. A measurement of >0.1 was determined as a cutoff for a positive result.

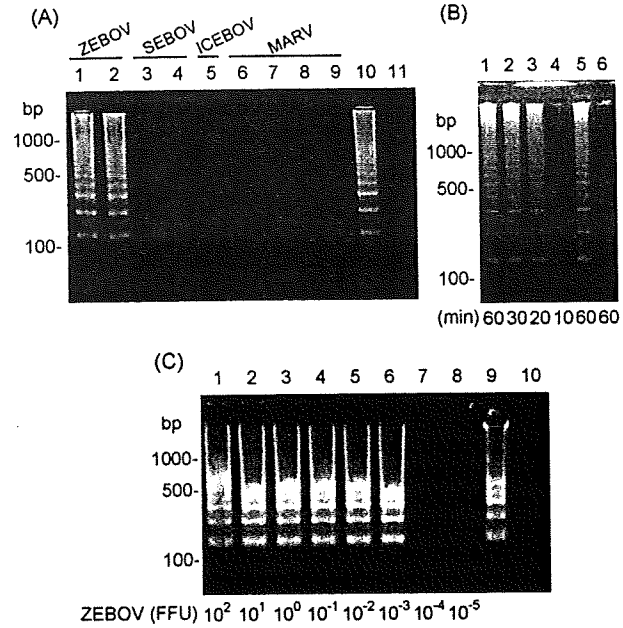

Fig. 4. Evaluation of RT-LAMP assay cell-culture propagated viral RNA. (A) Specificity of ZEBOV RT-LAMP. Each strain of filovirus was tested with RNA equivalent to 10^4 FFU. Lanes: 1, ZEBOV strain Mayinga; 2, ZEBOV strain Zaire 95; 3, SEBOV strain Boniface; 4, SEBOV strain Gulu; 5, ICEBOV; 6, MARV strain Musoke; 7, MARV strain Ozolin; 8, MARV strain Ravn; 9, MARV strain Angola; 10, 10^6 copies of in vitro transcribed ZEBOV RNA (positive control); 11, distilled water (negative control). (B) Time for detection of RT-LAMP assay. Aliquots of 10^4 FFU of ZEBOV strain Mayinga were tested in the assay. Each sample was amplified at 63 °C for the indicated times (Lanes 1–4). Lane 5, positive control; Lane 6, negative control. (C) Sensitivity of RT-LAMP assay. Tenfold serial dilution of viral RNA from ZEBOV strain Mayinga was used and RT-LAMP was carried out at 63 °C for 60 min. The concentrations of viral RNA are indicated (lanes 1–8). Lane 9, positive control; Lane 10, negative control. The positions of DNA size marker are shown on the left for each figure.

in Fig. 4A, only ZEBOV strains were detected, while SEBOV, ICEBOV, and MARV strains showed no amplification. Next, to determine the minimal time required to obtain the assay results, ZEBOV RNA was assayed for different durations as indicated in Fig. 4B. For 10^4 FFU of ZEBOV strain Mayinga, viral RNA could be amplified in 20 min, consistent with the results for in vitro transcribed ZEBOV RNA. Sensitivity of the RT-LAMP was determined using serial 10-fold dilutions of ZEBOV strain Mayinga RNA resulting in a limit of detection for this assay of 10^{-3} FFU (Fig. 4C).

4. Discussion

In this study, we developed an RT-LAMP assay specific for ZEBOV using primers spanning the 676 nt 5′ non-coding trailer sequence of the viral genome necessary for virus replication (Muhlberger et al., 1998, 1999; Sanchez and Rollin, 2005; Volchkov et al., 1999). In designing the primers, we compared the trailer sequence homologies of all filovirus strains available in GenBank. The sequences were highly conserved (more than 97%) among ZEBOV strains, but SEBOV and MARV (no trailer sequences for ICEBOV available in GenBank) trailer sequences showing much less homology. Thus, ZEBOV-specific RT-LAMP assay primers were designed.

Initial trials of this assay produced the characteristic ladder-like pattern of LAMP amplification upon gel electrophoresis and the identity of the product was confirmed by *Nsp*I digestion suggesting that the assay functioned as designed (Fig. 2A). The assay was next tested against a panel of filoviruses and did not show any cross-reactivity with human infectious other species of EBOV or MARV (Fig. 4A) as was expected. The utilization of four primers in LAMP assays allows for a very high degree of specificity to be employed as this result indicates.

The sensitivity of the assay was determined by amplification of 10-fold serial dilutions of both in vitro transcribed ZEBOV RNA and RNA from cell-culture propagated viruses. Reactions were positive at 20 copies of the in vitro transcribed RNA, and at 10^{-3} FFU from the intact virus (Fig. 2B, 3 and 4C). It has been reported that 10 RNA molecule standards could be detected by a TaqMan RT-PCR assay targeting the nucleoprotein gene (Weidmann et al., 2004), and a TaqMan RT-PCR targeting the GP gene was able to detect 10 fg and 8 PFU of purified ZEBOV RNA and infectious virus, respectively (Gibb et al., 2001). This RT-LAMP assay demonstrates almost equivalent or superior sensitivity to these RT-PCR methods, indicating that the sensitivity of RT-LAMP is sufficiently high to detect RNA in low copy numbers. The viral load profiles of patients with acute phase EHF caused by SEBOV in the Gulu outbreak indicated very high levels of genomic-sense RNA in samples from patients who died, sometimes reaching from 10^7 to 10^{10} RNA copies/mL of serum (Towner et al., 2004). LAMP is reported to be less influenced by PCR inhibitors in blood components (Al-Soud and Radstrom, 2001; Iwasaki et al., 2003) and with its high sensitivity, would be useful for clinical specimens such as blood or body fluids.

Real-time monitoring showed that the assay time required detecting ZEBOV viral RNA in samples was 16 or 26 min at concentrations of 2×10^6 or 20 copies, respectively (Fig. 3). These assay times are much shorter than those for conventional methods, such as real-time PCR and ELISA. The standard RT-PCR protocol, including reverse transcription, cDNA amplification, and detection, requires more than 60 min. In situations where rapid turnaround of results are necessary, such as outbreak management in Central Africa or in case of an intentional release, this rapid assay time would be of great benefit.

RT-LAMP has advantages over other nucleic acid amplification techniques in its simple operation and rapid detection. In the RT-LAMP assay, reverse transcription reaction and DNA amplification proceed in a single step and with incubation of the reaction mixture at 63 °C for a given period. The only equipment required for the LAMP reaction is a water bath or heat block that furnishes a constant temperature of 63 °C.

The assay we have developed in this study is as sensitive as other available technologies, highly specific and extremely rapid in the provision of molecular diagnosis of ZEBOV infections. These results indicate that similar RT-LAMP assay for the other EBOV species could be established with selecting appropriate target sequences. The assay does not require the use of sophisticated equipment or highly skilled personnel. The cost of the assay per sample is much lower than those of RT-PCR or ELISA and the assay can provide accurate results in a short time frame. This makes it potentially useful for clinical diagnosis of EBOV in developing countries or in cases of deliberate release during bioterrorism attacks.

Acknowledgements

We thank Toshie Sakuma and Aiko Fukuma for excellent technical assistance. This work was supported by grants from the Japan Science and Technology Agency (JST) and the Japan Society for the Promotion of Science (JSPS).

References

Al-Soud, W.A., Radstrom, P., 2001. Purification and characterization of PCR-inhibitory components in blood cells. J. Clin. Microbiol. 39, 485–493.

Ebihara, H., Yoshimatsu, K., Ogino, M., Araki, K., Ami, Y., Kariwa, H., Takashima, I., Li, D., Arikawa, J., 2000. Pathogenicity of Hantaan virus in newborn mice: genetic reassortant study demonstrating that a single amino acid change in glycoprotein G1 is related to virulence. J. Virol. 74, 9245–9255.

Feldmann, H., Volchkov, V.E., Volchkova, V.A., Stroher, U., Klenk, H.D., 2001. Biosynthesis and role of filoviral glycoprotein. J. Gen. Virol. 82, 2839–2848.

Feldmann, H., Geisbert, T.W., Jahrling, P.B., Klenk, H.D., Netesov, S.V., Peters, C.J., Sanchez, A., Swanepoel, R., Volchkov, V.E., 2004. Filoviridae. In: Fauquet, C.M., Mayo, M.A., Maniloff, J., Desselberger, U., Ball, L.A. (Eds.), Virus Taxonomy: Eighth Report of the International Committee on Taxonomy of Viruses. Elsevier Academic Press, San Diego, pp. 645–653.

Fisher-Hoch, S.P., Perez-Oronoz, P.I., Jackson, E.L., Hermann, L.M., Brown, B.G., 1992. Filovirus clearance in non-human primates. Lancet 340, 451–453.

Gibb, T.R., Norwood Jr., D.A., Woollen, N., Henchal, E.A., 2001. Development and evaluation of a fluorogenic 5′ nuclease assay to detect and differentiate between Ebola virus subtypes Zaire and Sudan. J. Clin. Microbiol. 39, 4125–4130.

Grolla, A., Lucht, A., Dick, D., Strong, J.E., Feldmann, H., 2005. Laboratory diagnosis of Ebola and Marburg hemorrhagic fever. Bull. Soc. Pathol. Exot. 98, 205–209.

Iwasaki, M., Yonekawa, T., Otsuka, K., Suzuki, W., Nagamine, K., Hase, T., Tatsumi, K.-I., Horigome, T., Notomi, T., Kanda, H., 2003. Validation of the loop-mediated isothermal amplification method for single nucleotide polymorphism genotyping with whole blood. Genome Lett. 2, 119–126.

Ksiazek, T.G., Rollin, P.E., Jahrling, P.E., Johnson, E., Dalgard, D.W., Peters, C.J., 1992. Enzyme immunosorbent assay for Ebola virus antigens in tissues of infected primates. J. Clin. Microbiol. 30, 947–950.

Ksiazek, T.G., Rollin, P.E., Williams, A.J., Bressler, D.S., Martin, M.L., Swanepoel, R., Burt, F.J., Leman, P.A., Khan, A.S., Rowe, A.K., Mukunu, R., Sanchez, A., Peters, C.J., 1999a. Clinical virology of Ebola hemorrhagic fever (EHF): virus, virus antigen, and IgG and IgM antibody findings among EHF patients in Kikwit, Democratic Republic of the Congo, 1995. J. Infect. Dis. 179 (Suppl. 1), S177–S187.

Ksiazek, T.G., West, C.P., Rollin, P.E., Jahrling, P.E., Peters, C.J., 1999b. ELISA for the detection of antibodies to Ebola viruses. J. Infect. Dis. 179 (Suppl. 1), S192–S198.

Leroy, E.M., Baize, S., Lu, C.Y., McCormick, J.B., Georges, A.J., Georges-Courbot, M.C., Lansoud-Soukate, J., Fisher-Hoch, S.P., 2000. Diagnosis of Ebola haemorrhagic fever by RT-PCR in an epidemic setting. J. Med. Virol. 60, 463–467.

Lloyd, E.S., Zaki, S.R., Rollin, P.E., Tshioko, K., Bwaka, M.A., Ksiazek, T.G., Calain, P., Shieh, W.J., Konde, M.K., Verchueren, E., Perry, H.N., Manguindula, L., Kabwau, J., Ndambi, R., Peters, C.J., 1999. Long-term disease surveillance in Bandundu region, Democratic Republic of the Congo: a model for early detection and prevention of Ebola hemorrhagic fever. J. Infect. Dis. 179 (Suppl. 1), S274–S280.

Mahanty, S., Bray, M., 2004. Pathogenesis of filoviral haemorrhagic fevers. Lancet Infect. Dis. 4, 487–498.

Mori, Y., Kitao, M., Tomita, N., Notomi, T., 2004. Real-time turbidimetry of LAMP reaction for quantifying template DNA. J. Biochem. Biophys. Methods 59, 145–157.

Muhlberger, E., Lotfering, B., Klenk, H.D., Becker, S., 1998. Three of the four nucleocapsid proteins of Marburg virus, NP, VP35, and L, are sufficient to mediate replication and transcription of Marburg virus-specific monocistronic minigenomes. J. Virol. 72, 8756–8764.

Muhlberger, E., Weik, M., Volchkov, V.E., Klenk, H.D., Becker, S., 1999. Comparison of the transcription and replication strategies of marburg virus and Ebola virus by using artificial replication systems. J. Virol. 73, 2333–2342.

Niikura, M., Ikegami, T., Saijo, M., Kurane, I., Miranda, M.E., Morikawa, S., 2001. Detection of Ebola viral antigen by enzyme-linked immunosorbent assay using a novel monoclonal antibody to nucleoprotein. J. Clin. Microbiol. 39, 3267–3271.

Notomi, T., Okayama, H., Masubuchi, H., Yonekawa, T., Watanabe, K., Amino, N., Hase, T., 2000. Loop-mediated isothermal amplification of DNA. Nucleic Acids Res. 28, E63.

Parida, M., Posadas, G., Inoue, S., Hasebe, F., Morita, K., 2004. Real-time reverse transcription loop-mediated isothermal amplification for rapid detection of West Nile virus. J. Clin. Microbiol. 42, 257–263.

Poon, L.L., Leung, C.S., Tashiro, M., Chan, K.H., Wong, B.W., Yuen, K.Y., Guan, Y., Peiris, J.S., 2004. Rapid detection of the severe acute respiratory syndrome (SARS) coronavirus by a loop-mediated isothermal amplification assay. Clin. Chem. 50, 1050–1052.

Saijo, M., Niikura, M., Morikawa, S., Ksiazek, T.G., Meyer, R.F., Peters, C.J., Kurane, I., 2001. Enzyme-linked immunosorbent assays for detection of antibodies to Ebola and Marburg viruses using recombinant nucleoproteins. J. Clin. Microbiol. 39, 1–7.

Sanchez, A., Trappier, S.G., Mahy, G.W., Peters, C.J., Nichol, S.T., 1996. The virion glycoproteins of Ebola viruses are encoded in two reading frames and are expressed through transcriptional editing. Proc. Natl. Acad. Sci. 93, 3602–3607.

Sanchez, A., Rollin, P.E., 2005. Complete genome sequence of an Ebola virus (Sudan species) responsible for a 2000 outbreak of human disease in Uganda. Virus Res. 113, 16–25.

Towner, J.S., Rollin, P.E., Bausch, D.G., Sanchez, A., Crary, S.M., Vincent, M., Lee, W.F., Spiropoulou, C.F., Ksiazek, T.G., Lukwiya, M., Kaducu, F., Downing, R., Nichol, S.T., 2004. Rapid diagnosis of Ebola hemorrhagic fever by reverse transcription-PCR in an outbreak setting and assessment of patient viral load as a predictor of outcome. J. Virol. 78, 4330–4341.

Volchkov, V.E., Volchkova, V.A., Chepurnov, A.A., Blinov, V.M., Dolnik, O., Netesov, S.V., Feldmann, H., 1999. Characterization of the L gene and 5' trailer region of Ebola virus. J. Gen. Virol. 80 (Pt 2), 355–362.

Watanabe, S., Watanabe, T., Noda, T., Takada, A., Feldmann, H., Jasenosky, L.D., Kawaoka, Y., 2004. Production of novel ebola virus-like particles from cDNAs: an alternative to ebola virus generation by reverse genetics. J. Virol. 78, 999–1005.

Weidmann, M., Muhlberger, E., Hufert, F.T., 2004. Rapid detection protocol for filoviruses. J. Clin. Virol. 30, 94–99.

Zaki, S.R., Shieh, W.J., Greer, P.W., Goldsmith, C.S., Ferebee, T., Katshitshi, J., Tshioko, F.K., Bwaka, M.A., Swanepoel, R., Calain, P., Khan, A.S., Lloyd, E., Rollin, P.E., Ksiazek, T.G., Peters, C.J., 1999. A novel immunohistochemical assay for the detection of Ebola virus in skin: implications for diagnosis, spread, and surveillance of Ebola hemorrhagic fever. Commission de Lutte contre les Epidemies a Kikwit. J. Infect. Dis. 179 (Suppl. 1), S36–S47.

Molecular phylogeny of a newfound hantavirus in the Japanese shrew mole (*Urotrichus talpoides*)

Satoru Arai*, Satoshi D. Ohdachi†, Mitsuhiko Asakawa‡, Hae Ji Kang§, Gabor Mocz¶, Jiro Arikawa‖, Nobuhiko Okabe*, and Richard Yanagihara§**

*Infectious Disease Surveillance Center, National Institute of Infectious Diseases, Tokyo 162-8640, Japan; †Institute of Low Temperature Science, Hokkaido University, Sapporo 060-0819, Japan; ‡School of Veterinary Medicine, Rakuno Gakuen University, Ebetsu 069-8501, Japan; §John A. Burns School of Medicine, University of Hawaii at Manoa, Honolulu, HI 96813; ¶Pacific Biosciences Research Center, University of Hawaii at Manoa, Honolulu, HI 96822; and ‖Institute for Animal Experimentation, Hokkaido University, Sapporo 060-8638, Japan

Communicated by Ralph M. Garruto, Binghamton University, Binghamton, NY, September 10, 2008 (received for review August 8, 2008)

Recent molecular evidence of genetically distinct hantaviruses in shrews, captured in widely separated geographical regions, corroborates decades-old reports of hantavirus antigens in shrew tissues. Apart from challenging the conventional view that rodents are the principal reservoir hosts, the recently identified soricid-borne hantaviruses raise the possibility that other soricomorphs, notably talpids, similarly harbor hantaviruses. In analyzing RNA extracts from lung tissues of the Japanese shrew mole (*Urotrichus talpoides*), captured in Japan between February and April 2008, a hantavirus genome, designated Asama virus (ASAV), was detected by RT-PCR. Pairwise alignment and comparison of the S-, M-, and L-segment nucleotide and amino acid sequences indicated that ASAV was genetically more similar to hantaviruses harbored by shrews than by rodents. However, the predicted secondary structure of the ASAV nucleocapsid protein was similar to that of rodent- and shrew-borne hantaviruses, exhibiting the same coiled-coil helix at the amino terminus. Phylogenetic analyses, using the maximum-likelihood method and other algorithms, consistently placed ASAV with recently identified soricine shrew-borne hantaviruses, suggesting a possible host-switching event in the distant past. The discovery of a mole-borne hantavirus enlarges our concepts about the complex evolutionary history of hantaviruses.

host switching | talpid | evolution | Japan

Dating from investigations conducted independently by Japanese and Russian medical scientists along opposite sides of the Amur River in the 1930s and 1940s, rodents have been suspected to harbor the etiological agent(s) of hemorrhagic fever with renal syndrome (HFRS) (1, 2). After a several decades-long impasse, the striped field mouse (*Apodemus agrarius*) was identified as the reservoir host of Hantaan virus (3), the prototype virus of HFRS (4). This seminal discovery made possible the identification of genetically distinct hantaviruses in other murinae and arvicolinae rodent species (5–12). Also, a previously unrecognized, frequently fatal respiratory disease, called hantavirus pulmonary syndrome (HPS) (13), is now known to be caused by hantaviruses harbored by neotominae and sigmodontinae rodents in the Americas, the prototype being Sin Nombre virus (SNV) in the deer mouse (*Peromyscus maniculatus*) (14). Remarkably, each of these hantaviruses appears to share a long coevolutionary history with a specific rodent host species. That is, based on phylogenetic analyses of full-length viral genomic and rodent mitochondrial DNA (mtDNA) sequences, these hantaviruses segregate into clades, which parallel the evolution of rodents in the murinae, arvicolinae, neotominae, and sigmodontinae subfamilies (15, 16).

Until recently, the single exception to the strict rodent association of hantaviruses was Thottapalayam virus (TPMV), a long-unclassified virus originally isolated from the Asian house shrew (*Suncus murinus*) (17, 18). Analysis of the recently acquired full genome of TPMV strongly supports an ancient non-rodent host origin and an early evolutionary divergence from rodent-borne hantaviruses (19, 20). Employing RT-PCR and oligonucleotide primers based on the TPMV genome, we have targeted the discovery of hantaviruses in shrew species from widely separated geographical regions, including the Chinese mole shrew (*Anourosorex squamipes*) from Vietnam (21), Eurasian common shrew (*Sorex araneus*) from Switzerland (22), northern short-tailed shrew (*Blarina brevicauda*), masked shrew (*Sorex cinereus*), and dusky shrew (*Sorex monticolus*) from the United States (23, 24) and Ussuri white-toothed shrew (*Crocidura lasiura*) from Korea (J.-W. Song and R. Yanagihara, unpublished observations). Many more shrew-hantavirus associations undoubtedly exist, as evidenced by preliminary studies of *Sorex caecutiens* and *Sorex roboratus* from Russia (H. J. Kang, S. Arai and R. Yanagihara, unpublished observations) and *Sorex palustris*, *Sorex trowbridgii*, and *Sorex vagrans* from North America (H. J. Kang and R. Yanagihara, unpublished observations).

In addition to challenging the view that rodents are the sole or principal reservoirs of hantaviruses, the discovery of soricid-borne hantaviruses predicts that other soricomorphs, notably talpids, might also harbor genetically distinct hantaviruses. In this regard, hantavirus antigens have been detected by enzyme immunoassay and fluorescence techniques in tissues of the European common mole (*Talpa europea*) captured in Russia (25) and Belgium (26), but no reports are available about hantavirus infection in shrew moles. Relying on oligonucleotide primers designed from our expanding sequence database of shrew-borne hantaviruses, we have identified a hantavirus genome, designated Asama virus (ASAV), in the Japanese shrew mole (*Urotrichus talpoides*). Genetic and phylogenetic analyses indicate that ASAV is distinct but related to hantaviruses harbored by Old World soricine shrews, suggesting a very ancient evolutionary history, probably involving multiple host-switching events in the distant past.

Results

RT-PCR Detection of Hantavirus Sequences. In using RT-PCR to analyze RNA extracts, from lung tissues of three Laxmann's shrew (*Sorex caecutiens*), five slender shrew (*Sorex gracillimus*), six long-clawed shrew (*Sorex unguiculatus*), one dsinezumi shrew (*Crocidura dsinezumi*), and six Japanese shrew mole (*Urotrichus talpoides*), hantavirus sequences were not detected in shrew tissues, but were found in one of two and in two of three Japanese shrew moles (Fig. 1), captured in Ohtani (34 28′14.0° N; 136 45′46.2° E) and near

Author contributions: S.A. and R.Y. designed research; S.A., S.D.O., M.A., J.A., N.O., and R.Y. performed research; S.A. and H.J.K. contributed new reagents/analytic tools; S.A., S.D.O., H.J.K., G.M., and R.Y. analyzed data; and S.A., G.M., J.A., and R.Y. wrote the paper.

The authors declare no conflict of interest.

Freely available online through the PNAS open access option.

Data deposition: The sequences reported in this paper have been deposited in the GenBank database [accession numbers: ASAV S segment (EU929070, EU929071, EU929072); ASAV M segment (EU929073, EU929074, EU929075); and ASAV L segment (EU929076, EU929077, EU929078].

**To whom correspondence should be addressed at: John A. Burns School of Medicine, University of Hawaii at Manoa, 651 Ilalo Street, BSB 320L, Honolulu, HI 96813. E-mail: yanagiha@pbrc.hawaii.edu.

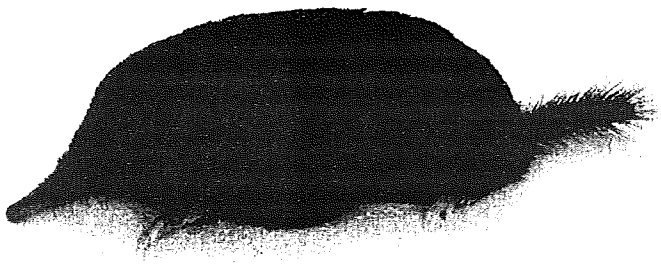

Fig. 1. Japanese shrew mole (*Urotrichus talpoides*) (family *Talpidae*, subfamily Talpinae), one of two endemic shrew mole species found only in Japan.

Asama River (34 28′12.79° N; 136 45′45.81° E), respectively, located approximately 1 km apart at an elevation of 50 m in Mie Prefecture, during February and April 2008. After the initial detection of hantavirus sequences, amplification of the S-, M-, and L-genomic segments was accomplished by using oligonucleotide primers based on conserved regions.

Nucleotide and Amino Acid Sequence Analysis. The S, M, and L segments of ASAV, as amplified from tissues of three wild-caught Japanese shrew moles, indicated an overall genomic structure similar to that of other rodent- and soricid-borne hantaviruses. The nucleotide and deduced-amino acid sequences of each ASAV genomic segment were highly divergent from that of rodent-borne hantaviruses, differing by approximately 30–40% (Table 1).

The S-genomic segment of ASAV (1,801 nucleotides for strains H4 and N9 and 1,756-nucleotides for strain N10) encoded a predicted nucleocapsid (N) protein of 434 amino acids, starting at nucleotide position 39, and a 3′-noncoding region (NCR) of approximately 465 nucleotides. The hypothetical NSs opening reading frame, typically found in the S segment of arvicolinae, neotominae, and sigmodontinae rodent-borne hantaviruses, was not found in ASAV. The interstrain variation of the S segment among the ASAV strains was negligible (1.1% at the nucleotide and 0% at the amino acid levels). In the hypervariable region of the N protein, between amino acid residues 244 and 269, ASAV differed by 18–20 and 20–22 amino acid from soricine shrew- and rodent-borne hantaviruses, respectively. Sequence similarity of the entire S-genomic segment of ASAV strains H4, N9, and N10 was higher with soricine shrew-borne hantaviruses than with hantaviruses harbored by rodents (Table 1).

Table 1. Nucleotide and amino acid sequence similarity (%) between ASAV strain N10 and representative rodent- and shrew-borne hantaviruses

	S segment		M segment		L segment	
Virus strain	1710 nt	434 aa	3604 nt	1141 aa	6126 nt	2041aa
HTNV 76–118	58.5	62.7	62.7	59.4	70.3	74.6
SEOV 80–39	63.1	62.0	62.8	59.1	70.4	74.7
SOOV SOO-1	62.8	62.9	63.3	59.7	70.2	74.3
DOBV Greece	62.2	62.2	63.0	59.3	70.2	75.7
PUUV Sotkamo	59.3	59.3	59.6	52.2	68.1	68.0
TULV 5302v	61.5	59.4	60.5	52.6	68.3	67.9
PHV PH-1	60.7	59.3	59.3	51.9	66.4	67.1
SNV NMH10	60.9	58.9	59.0	54.1	68.2	68.8
RPLV MSB89866	—	—	68.8	63.5	75.2	83.2
CBNV CBN-3	67.7	70.4	68.2	71.0	76.0	84.7
ARRV MSB73418	65.7	66.6	70.9	77.0	73.8	83.5
JMSV MSB89332	66.2	66.9	—	—	74.3	82.6
SWSV mp70	63.8	69.9	75.2	79.5	75.0	83.2
ASAV H4	98.9	100	99.3	99.6	98.2	99.6
ASAV N9	100	100	99.9	100	100	100
MJNV 05–11	57.2	46.0	56.1	44.4	65.8	61.5
TPMV VRC	58.0	45.8	57.7	43.0	64.3	62.0

Abbreviations: ARRV, Ash River virus; ASAV, Asama virus; CBNV, Cao Bang virus; DOBV, Dobrava virus; HTNV, Hantaan virus; JMSV, Jemez Spring virus; MJNV, Imjin virus; PHV, Prospect Hill virus; PUUV, Puumala virus; RPLV, Camp Ripley virus; SEOV, Seoul virus; SNV, Sin Nombre virus; SOOV, Soochong virus; SWSV, Seewis virus; TPMV, Thottapalayam virus; TULV, Tula virus. nt, nucleotides; aa, amino acids.

The 3,646-nucleotide full-length M-genomic segment of ASAV encoded a predicted glycoprotein of 1,141 amino acids, starting at nucleotide position 41, and a 183-nucleotide 3′-NCR. Four potential N-linked glycosylation sites (three in Gn at amino acid positions 138, 352, 404, and one in Gc at position 933) were found in ASAV. In addition, the highly conserved WAASA amino acid motif, which in ASAV was WAVSA (amino acid positions 649–653), was present. An interstrain variation of 0.1–0.7% and 0–0.4% at the nucleotide and amino acid levels, respectively, was found among ASAV strains H4, N9, and N10. The full-length Gn/Gc amino acid sequence of ASAV exhibited the highest similarity with Seewis virus (79.5%) from the Eurasian common shrew (Table 1).

Analysis of the nearly full-length 6,126-nucleotide (2,041-amino acid) L segment of ASAV revealed the five conserved motifs (A–E), identified among all hantavirus RNA polymerases. The overall high sequence similarity of the L segment among ASAV and rodent- and soricid-borne hantaviruses was consistent with the functional constraints on the RNA-dependent RNA polymerase (Table 1).

Secondary Structure of N Protein. Secondary structure analysis revealed striking similarities, as well as marked differences, among the N protein sequences of ASAV and 13 representative rodent- and soricid-hantaviruses. Each sequence appeared to adopt a two-domain, predominantly α-helical structure joined by a central β-pleated sheet. Whereas the length of the N-terminal domain was mostly invariant, the length of the central β-pleated sheet and of the adjoining C-terminal α-helical domain showed systematic reciprocal structural changes according to the genetic relationship and evolutionary descent of the individual sequences.

The N-terminal α-helical domain, from residues 1 to approximately 140, was composed of four helices connected by large loops (representative viruses shown in Fig. 2). The C-terminal α-helical domain, from residues 210/230 to 430, contained seven to nine helices that were connected by tighter loops (Fig. 2). And the central β-pleated region, from residues 140 to 210/230, was composed of three to five possible anti-parallel strands. Interestingly, an increasing number of strands in this section were observed when the hantaviral sequences were arranged according to their positions in the phylogenetic tree. This resulted in a widening of the central β-pleated region with a concomitant shortening of the C-terminal α-helical domain while preserving the total length of the protein. The helix adjoining the central β-sheet progressively shortened in this architectural change. These structural alterations were reversed in TPMV, which was evolutionarily more distant from the other sequences (Fig. 2).

Phylogenetic Analysis. Exhaustive phylogenetic analyses based on nucleotide and deduced amino acid sequences of the S-, M-, and L-genomic segments, generated by the maximum-likelihood (ML) method, indicated that ASAV was distinct from rodent-borne hantaviruses (with high posterior node probabilities based on 30,000 trees) (Fig. 3). Nearly identical topologies were consistently derived, by using various algorithms and different taxa and combinations of taxa, suggesting an ancient evolutionary origin. The most strikingly consistent feature was the phylogenetic position of ASAV with soricine shrew-borne hantaviruses, rather than being placed as an outgroup beyond TPMV, the prototype crocidurine shrew-borne hantavirus. That is, the prediction that a shrew mole-associated hantavirus would be phylogenetically distant from hantaviruses harbored by shrews was not validated.

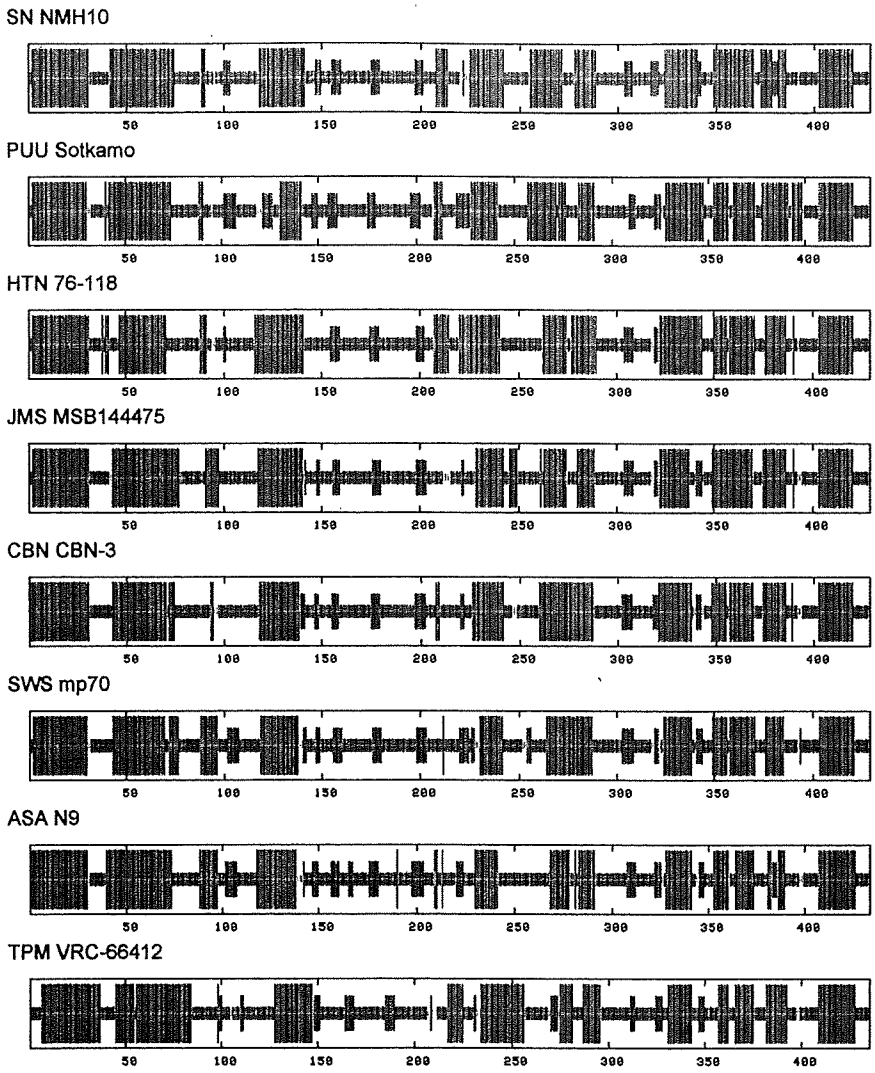

Fig. 2. Consensus secondary structure of N protein of ASAV and representative rodent- and soricid-borne hantaviruses, predicted using a high-performance method implemented on the NPS@ structure server (47). As shown, the ASAV N protein was very similar to that of other hantaviruses, characterized by the same coiled-coil helix at the amino terminal end and similar secondary structure motifs at their carboxyl terminals. The predicted structures were represented by colored bars to visualize the schematic architecture: α-helix, blue; β-sheet, red; coil, magenta; unclassified, gray. For simplicity, turns and other less frequently occurring secondary structural elements were omitted. All sequences are numbered from Met-1.

Sequence and Phylogenetic Analysis of Mole mtDNA. Molecular confirmation of the taxonomic identification of the hantavirus-infected Japanese shrew moles based on morphological features was achieved by amplification and sequencing of the 1,140-nucleotide mtDNA cytochrome *b* gene. Phylogenetic analysis showed distinct grouping of hantavirus-infected *U. talpoides* from this study with other *U. talpoides* mtDNA sequences available in GenBank, rather than with soricids or rodents (Fig. 4).

Discussion

Newfound Shrew Mole-Borne Hantavirus. Despite reports of hantavirus antigens in tissues of the Eurasian common shrew (*Sorex araneus*), alpine shrew (*Sorex alpinus*), Eurasian water shrew (*Neomys fodiens*), and common mole (*Talpa europea*) (25–28), shrews and moles have been generally dismissed as being unimportant in the transmission dynamics of hantaviruses. With the recent demonstration that TPMV and other newly identified soricid-borne hantaviruses are genetically distinct and phylogenetically distant from rodent-borne hantaviruses (19–24), the conventional view that rodents are the principal or primordial reservoir hosts of hantaviruses is being challenged. In its wake, a compelling conceptual framework, or paradigm shift, is emerging that supports an ancient origin of hantaviruses in soricomorphs (or insectivores). To this emerging concept must now be added the first molecular evidence of a newfound hantavirus, designated ASAV, in the Japanese shrew mole (family *Talpidae*, subfamily *Talpinae*). The demonstration of ASAV sequences in this endemic shrew mole species captured at different times and in two separate locations in Mie Prefecture argues strongly against this being an isolated or coincidental event. Instead, these data suggest a well established coexistence of this newfound hantavirus in the Japanese shrew mole and further solidifies the notion of a long-standing evolutionary association between soricomorphs and hantaviruses.

Shrew moles differ from typical or true moles in that they look like shrews and are much less specialized for burrowing. The greater Japanese shrew mole, which morphologically resembles semifossorial shrew moles in China (*Scaptonyx*) and North America (*Neurotrichus*), is widely distributed in the lowlands and peripheral islands of Japan, except Hokkaido, and is not found on mainland Asia (29, 30). Also endemic in Japan, the lesser Japanese shrew mole (*Dymecodon pilirostris*) is largely restricted to mountainous regions on Honshu, Shikoku, and Kyushu and is considered the more ancestral species. As determined by cytochrome *b* mtDNA and nuclear recombination activating gene-1 (RAG1) sequence analyses, the greater and lesser Japanese shrew moles are closely related, but their evolutionary origins and biogeography remain unresolved (31, 32). The existence of two distinct chromosomal races of *U. talpoides*, geographically separated by the Fuji and Kurobe rivers in central Honshu (33, 34), provides an opportunity to further clarify the evolutionary origins of shrew mole-borne hantaviruses in Japan. Studies, now underway, will examine whether ASAV is harbored by *U. talpoides* in locations east of Mie

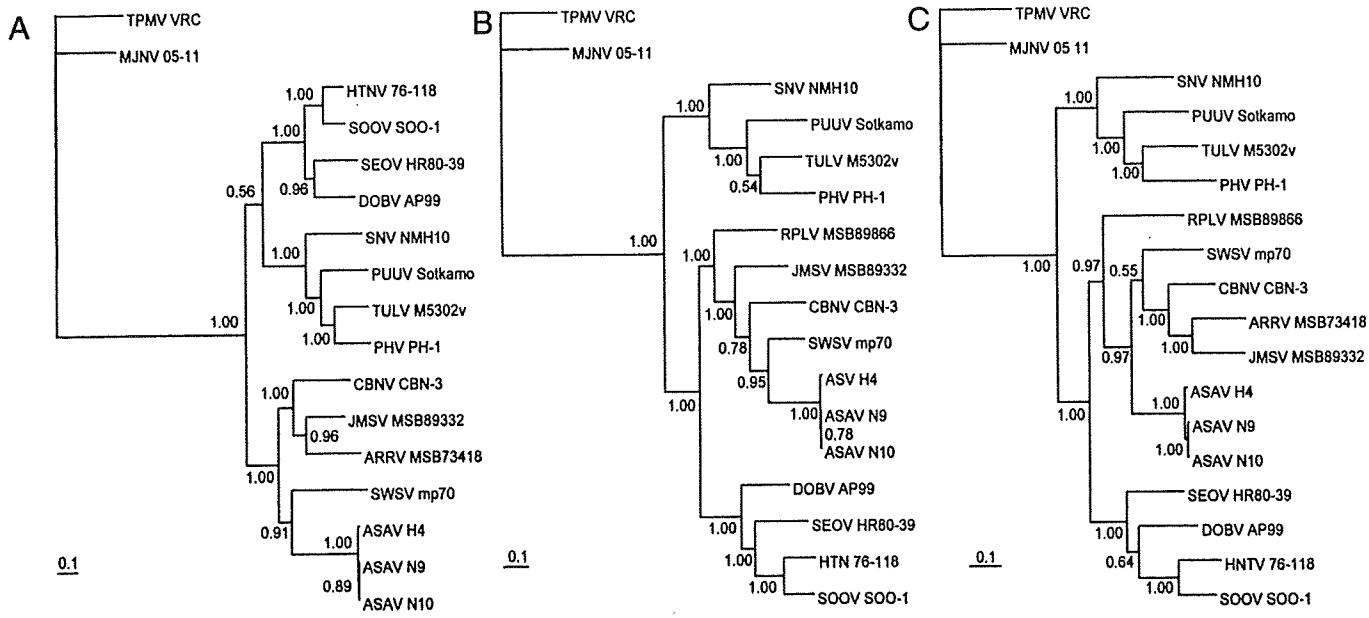

Fig. 3. Phylogenetic trees generated by the ML method, using the GTR+I+G model of evolution as estimated from the data, based on the alignment of the coding regions of the full-length (*A*) 1,302-nucleotide S and (*B*) 3,423-nucleotide M segments, and partial (*C*) 6,126-nucleotide L-genomic segment of ASAV. The phylogenetic positions of ASAV strains H4, N9, and N10 are shown in relationship to representative murinae rodent-borne hantaviruses, including Hantaan virus (HTNV 76–118, NC_005218, NC_005219, NC_005222), Soochong virus (SOOV SOO-1, AY675349, AY675353, DQ056292), Dobrava virus (DOBV AP99, NC_005233, NC_005234, NC_005235), and Seoul virus (SEOV HR80–39, NC_005236, NC_005237, NC_005238); arvicolinae rodent-borne hantaviruses, including Tula virus (TULV M5302v, NC_005227, NC_005228, NC_005226), Puumala virus (PUUV Sotkamo, NC_005224, NC_005223, NC_005225), and Prospect Hill virus (PHV PH-1, Z49098, X55129, EF646763); and a neotominae rodent-borne hantavirus, Sin Nombre virus (SNV NMH10, NC_005216, NC_005215, NC_005217). Also shown are Thottapalayam virus (TPMV VRC, AY526097, EU001329, EU001330) from the Asian house shrew (*Suncus murinus*); Imjin virus (MJNV 05–11, EF641804, EF641798, EF641806) from the Ussuri white-toothed shrew (*Crocidura lasiura*); Cao Bang virus (CBNV CBN-3, EF543524, EF543526, EF543525) from the Chinese mole shrew (*Anourosorex squamipes*); Ash River virus (ARRV MSB 73418, EF650086, EF619961) from the masked shrew (*Sorex cinereus*); Jemez Springs virus (JMSV MSB89332, EF619962, EF619960) from the dusky shrew (*Sorex monticolus*); and Seewis virus (SWSV mp70, EF636024, EF636025, EF636026) from the Eurasian common shrew (*Sorex araneus*). The numbers at each node are posterior node probabilities based on 30,000 trees: two replicate MCMC runs consisting of six chains of 3 million generations each sampled every 1,000 generations with a burn-in of 7,500 (25%). The scale bar indicates nucleotide substitutions per site. GenBank accession numbers: ASAV S segment (H4, EU929070; N9, EU929071; N10, EU929072); ASAV M segment (H4, EU929073; N9, EU929074; N10, EU929075); and ASAV L segment (H4, EU929076; N9, EU929077; N10, EU929078).

Prefecture, as well as ascertain whether *D. pilirostris* also serves as a reservoir of ASAV-related hantaviruses.

Although our RT-PCR attempts have failed to detect hantavirus sequences in other talpid species, including the long-nosed mole (*Euroscaptor longirostris*) (21) and eastern mole (*Scalopus aquaticus*) (H. J. Kang, J.-W. Song, and R. Yanagihara, unpublished observations), it may be because appropriate primers were not used. That is, based on the vast genetic diversity of soricid-borne hantaviruses, talpid-associated hantaviruses may be even more highly divergent and would require designing very different primers for amplification.

Finally, as for shrew-borne hantaviruses, the importance of this newfound shrew mole-associated hantavirus to human health warrants careful inquiry. Virus isolation attempts have been unsuccessful to date. In the meantime, an ASAV recombinant N protein is being prepared for use in enzyme immunoassays. In this regard, as evidenced by the corresponding sequence of YIEVNGIRKP in the ASAV N protein, the monoclonal antibody E5/G6, which recognizes the epitope YEDVNGIRKP (with variations) in rodent-borne hantaviruses (35), might be useful as a capturing antibody. In addition, other sensitive technologies, including nucleic acid and protein microarrays, are being developed to establish whether ASAV is pathogenic for humans.

Secondary Structure of Hantavirus N Protein. The overall N protein secondary structure of ASAV and other hantaviruses was compatible with a putative bilobed, three-dimensional protein architecture, which would allow the protein to clamp around the RNA as often observed in a variety of RNA-binding proteins. Whereas the core elements of the central β-pleated sheet appeared also to be conserved, more evolutionary variability was seen in the number of constituent strands and in the adjoining connecting elements and helices. This variability may reflect the function of this region as a flexible spacer element that can determine the relative orientation and separation of the two main α-helical domains and can accommodate the conformational changes upon RNA binding. The connecting regions could act as hinges of variable size leading to opening of the nucleocapsid. The flexible domain linkage would allow the interaction with the differently sized virus-specific RNA structures may modulate the oligomerization or assembly of the N protein in an evolutionarily and systematically changing fashion.

Phylogeny of Hantaviruses. Just as the identification of novel hantaviruses in the Therese shrew (*Crocidura theresae*) (36) and the northern short-tailed shrew (*Blarina brevicauda*) (23) heralded the discovery of other soricid-borne hantaviruses (21, 22, 24), the detection of ASAV in the Japanese shrew mole forecasts the existence of other hantaviruses in talpids. Perhaps more importantly, these findings emphasize that the evolutionary history and transmission dynamics of hantaviruses are far more rich and complex than originally imagined. That is, instead of a single progenitor virus being introduced into the rodent lineage more than 50 million years ago, mounting evidence supports a more ancient virus lineage with parallel coevolution of hantaviruses in crocidurine and soricine shrews. And given the sympatric and synchronistic coexistence of moles, shrews, and rodents, through a long continuum dating from the distant past to the present time, it seems

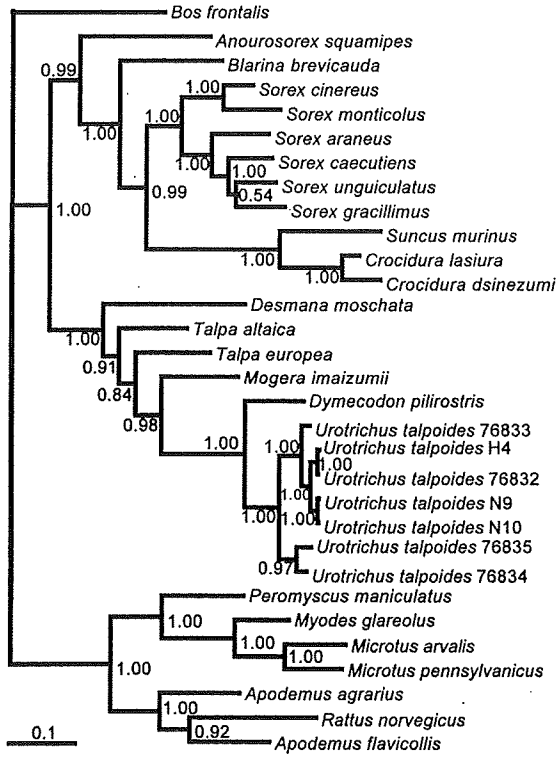

Fig. 4. Confirmation of host identification of ASAV-infected *Urotrichus talpoides* by mtDNA sequencing. Phylogenetic tree, based on the 1,140-nucleotide cytochrome *b* (cyt b) gene, was generated by the ML method. The phylogenetic positions of *Urotrichus talpoides* H4 (EU918369), N9 (EU918370), and N10 (EU918371) are shown in relationship to other *Urotrichus talpoides* cyt b sequences from GenBank (Ut76835: AB076835; Ut76834: AB076834; Ut76833: AB076833; Ut76832: AB076832), as well as other talpids, including *Desmana moschata* (AB076836), *Talpa altaica* (AB037602), *Talpa europea* (AB076829), *Mogera imaizumii* (AB037616), *Dymecodon pilirostris* (AB076830), and *Bos frontalis* (EF061237). Also shown are representative murinae rodents, including *Apodemus agrarius* (AB303226), *Apodemus flavicollis* (AB032853), and *Rattus norvegicus* (DQ439844); arvicolinae rodents, including *Microtus arvalis* (EU439459), *Myodes glareolus* (DQ090761), and *Microtus pennsylvanicus* (AF119279); and a neotominae rodent, *Peromyscus maniculatus* (AF119261), as well as crocidurinae shrews, including *Suncus murinus* (DQ630386), *Crocidura lasiura* (AB077071), and *Crocidura dsinezumi* (AB076837); and soricinae shrews, including *Anourosorex squamipes* (AB175091), *Blarina brevicauda* (DQ630416), *Sorex cinereus* (EU088305), *Sorex monticolus* (AB100273), *Sorex araneus* (DQ417719), *Sorex caecutiens* (AB028563), *Sorex unguiculatus* (AB028525), and *Sorex gracillimus* (AB175131). The numbers at each node are posterior node probabilities based on 30,000 trees: two replicate MCMC runs consisting of six chains of 3 million generations each sampled every 1,000 generations with a burn-in of 7,500 (25%). The scale bar indicates nucleotide substitutions per site.

plausible that ongoing exchanges of hantaviruses continues to drive their evolution.

In this regard, several rodent species may occasionally serve as reservoir hosts for the same hantavirus. For example, Vladivostok virus (VLAV) may be found in its natural host, the reed vole (*Microtus fortis*) (37–39), as well as an ancillary host, the tundra or root vole (*Microtus oeconomus*) (40). Similarly, the Maximowiczi vole (*Microtus maximowiczii*) is the natural reservoir of Khabarovsk virus (KHAV), which may also be harbored by *Microtus fortis* (10, 39, 40). Moreover, a KHAV-related hantavirus, named Topografov virus (TOPV), has also been found in the Siberian lemming (*Lemmus sibiricus*) (41). This is a far more extreme situation in which a hantavirus has switched from its natural rodent reservoir host and become well established in a rodent host of a different genus. Such host-switching or species-jumping events may account for the extraordinarily close phylogenetic relationship between TOPV and KHAV (41). That is, whereas *Lemmus* and *Microtus* are very distantly related, TOPV and KBRV are monophyletic.

In much the same way, as evidenced by the polyphylogenetic relationship between ASAV and other soricid-associated hantaviruses, the progenitor of ASAV may have 'jumped' from its natural soricine shrew host to establish itself in the Japanese shrew mole, or vice versa. That is, burrows and shallow tunnel systems excavated by Japanese shrew moles may be occasionally shared with sympatric species, including shrews, allowing opportunities for virus transmission through interspecies wounding or contaminated nesting materials. Such a host-switching event may have occurred in the distant past, possibly before the present-day Japanese shrew mole became endemic in Japan. Accordingly, intensive investigations of shrews in Japan and elsewhere in Far East Asia may provide further insights into the evolutionary origins of hantaviruses.

Materials and Methods

Trapping. Sherman traps (H.B. Sherman) and pit-hole traps were used to capture shrews and shrew moles in Japan between October 2006 and April 2008. Traps were set at intervals of 4 to 5 m during the evening hours of each day, over a four-day period, at sites in Hokkaido (Hamatonbetsu, Saruhutsu, and Nopporo) and Honshu (Nara and Mie), where soricomorphs had been captured. Species, gender, weight, reproductive maturity, and global positioning system (GPS) coordinates of each captured animal were recorded.

Specimen Processing. Lung tissues, dissected using separate instruments, were frozen on dry ice, and then stored at −80°C until used for testing. In some instances, portions of tissues were also placed in RNAlater RNA Stabilization Reagent (QIAGEN, Inc.) and processed for RT-PCR within 4 weeks of tissue collection.

RNA Extraction and cDNA Synthesis. Total RNA was extracted from tissues, by using the PureLink Microto-Midi total RNA purification kit (Invitrogen), in a laboratory in which hantaviruses had never been handled. cDNA was then prepared by using the SuperScript™ III RNase H- reverse transcriptase kit (Invitrogen) with a primer based on the conserved 5′-terminus of the S, M and L segments of hantaviruses (5′-TAGTAGTAGACTCC-3′).

RT-PCR. Touchdown-PCR was performed by using oligonucleotide primers designed from TPMV and other hantaviruses: S (outer: 5′-TAGTAGTAGACTCCT-TRAARAGC-3′ and 5′-AGCTCIGGATCCATITCATC-3′; inner: 5′-AGYCCIGTIATGRG-WGTIRTYGG-3′ and 5′-AIGAYTGRTARAAIGAIGAYTTYT T-3′); M (outer: 5′-GGACCAGGTGCADCTTGTGAAGC-3′ and 5′-GAACCCCADGCCCCITCYAT-3′; inner: 5′-TGTGTICCWGGITTYCATGGIT-3′ and 5′-CATGAYATCTCCAGGGTCHCC-3′); and L (outer: 5′-ATGTAYGTBAGTGCWGATGC-3′ and 5′-AACCADTCWGTYC-CRTCATC-3′; inner: 5′-TGCWGATGCHACIAARTGGTC-3′ and 5′-GCRTCRTCW-GARTGRTGDGCAA-3′).

First- and second-round PCR were performed in 20-μL reaction mixtures, containing 250 μM dNTP, 2.5 mM $MgCl_2$, 1 U of LA Taq polymerase (Takara) and 0.25 μM of each primer (24). Initial denaturation at 94°C for 2 min was followed by two cycles each of denaturation at 94°C for 30 sec, two-degree step-down annealing from 46°C to 38°C for 40 sec, and elongation at 72°C for 1 min, then 30 cycles of denaturation at 94°C for 30 sec, annealing at 42°C for 40 sec, and elongation at 72°C for 1 min, in a GeneAmp PCR 9700 thermal cycler (Perkin–Elmer). PCR products were separated by agarose gel electrophoresis and purified by using the Qiaex Gel Extraction Kit (Qiagen). Amplified DNA was sequenced directly by using an ABI Prism 3130 Avant Genetic Analyzer (Applied Biosystems).

Genetic and Phylogenetic Analyses. Sequences were processed by using the Genetyx version 9 software (Genetyx Corporation) and aligned using Clustal W and W2 (42). For phylogenetic analysis, ML consensus trees were generated by the Bayesian Metropolis–Hastings Markov Chain Monte Carlo (MCMC) tree-sampling methods as implemented by Mr. Bayes (43) using a GTR+I+G model of evolution, as selected by hierarchical likelihood-ratio test (hLRT) in MrModeltest2.3 (http://www.abc.se/~nylander/mrmodeltest2/mrmodeltest2.html) (44), partitioned by codon position.

An initial ML estimate of the model of evolutionary change among aligned viruses was generated by MrModeltest2.3. ML tree estimation in PAUP (45) was conducted starting with a neighbor-joining (NJ) tree based on this initial ML model of evolution, and proceeding with successive rounds of heuristic tree-searches to select the single most likely ML tree. Support for topologies was generated by bootstrapping for 1,000 NJ replicates (under the ML model of evolution, implemented in

PAUP) and for 100 ML replicates (data not shown). Phylogenetic relationships were further confirmed using amino acid sequences analyzed by Bayesian tree sampling, using the WAG model (46) implemented by Bayes (43).

Secondary Structure Prediction. Secondary structure prediction of the N protein was performed using the NPS@ structure server (47). To achieve 70–80% accuracy and to validate the prediction, five different methods were used jointly: DSC (48), HNN (49), PHD (50), PREDATOR (51), and MLRC (49), which in turn were based on GOR4 (52), SIMPA96 (53), and SOPMA (54). The minimum number of conformational states was set to four (helix, sheet, turn, and coil) for each analysis, and the results were combined into a consensus structure where the most prevalent predicted conformational state was reported for each residue. For convenience in visualization of the predicted structures, the NPS@ server also provided graphic outputs for the individual sequences which were subsequently combined into a multipart joint image.

PCR Amplification of Shrew Mole mtDNA. Total DNA, extracted from liver tissues using the QIAamp Tissue Kit (QIAGEN), was used to verify the identity of the hantavirus-infected shrew moles. The 1,140-nucleotide mtDNA cytochrome *b* gene was amplified by PCR, using described universal primers (5′- CGAAGCTT-GATATGAAAAACCATCGTTG-3′; 5′- AACTGCAGTCATCTCCGGTTTACAAGAC-3′) (55). PCR was performed in 50-μl reaction mixtures, containing 200 μM dNTP and 1.25 U of rTaq polymerase (Takara). Cycling conditions consisted of an initial denaturation at 95°C for 4 min followed by 40 cycles with denaturation at 94°C for 1 min, annealing at 57°C for 1 min, and elongation at 72°C for 1 min in a GeneAmp PCR9700 thermal cycler.

ACKNOWLEDGMENTS. We thank Dr. Akio Shinohara (Frontier Science Research Center, University of Miyazaki) for kindly providing the photo of the Japanese shrew mole (Fig. 1). This work was supported by a Grant-in-Aid for Scientific Research (B) from the Ministry of Education, Science, and Culture of Japan (18300136), Gakujyutsu-Frontier Cooperative Research at Rakuno Gakuen University, and National Institute of Allergy and Infectious Diseases Grant R01AI075057, Centers of Biomedical Research Excellence Grant P20RR018727, and Research Centers in Minority Institutions Grant G12RR003061 from the National Center for Research Resources, National Institutes of Health.

1. Yanagihara R (1990) Hantavirus infection in the United States: Epizootiology and epidemiology. *Rev Infect Dis* 12:449–457.
2. Yanagihara R, Gajdusek DC (1988) in *CRC Handbook of Viral and Rickettsial Hemorrhagic Fevers*, ed Gear JHS (CRC Press, Boca Raton), pp 151–188.
3. Lee HW, Lee P-W, Johnson KM (1978) Isolation of the etiologic agent of Korean hemorrhagic fever. *J Infect Dis* 137:298–308.
4. Schmaljohn CS, Hasty SE, Harrison SA, Dalrymple JM (1983) Characterization of Hantaan virions, the prototype virus of hemorrhagic fever with renal syndrome. *J Infect Dis* 148:1005–1012.
5. Brummer-Korvenkontio M, *et al.* (1980) Nephropathia epidemica: Detection of antigen in bank voles and serologic diagnosis of human infection. *J Infect Dis* 141:131–134.
6. Lee HW, Baek LJ, Johnson KM (1982) Isolation of Hantaan virus, the etiologic agent of Korean hemorrhagic fever from wild urban rats. *J Infect Dis* 146:638–644.
7. Lee P-W, *et al.* (1985) Partial characterization of Prospect Hill virus isolated from meadow voles in the United States. *J Infect Dis* 152:826–829.
8. Avsic-Zupanc T, *et al.* (1992) Characterization of Dobrava virus: A hantavirus from Slovenia, Yugoslavia. *J Med Virol* 38:132–137.
9. Plyusnin A, *et al.* (1994) Tula virus: A newly detected hantavirus carried by European common voles. *J Virol* 68:7833–7839.
10. Hörling J, *et al.* (1996) Khabarovsk virus: A phylogenetically and serologically distinct hantavirus isolated from *Microtus fortis* trapped in far-east Russia. *J Gen Virol* 77:687–694.
11. Nemirov K, *et al.* (1999) Isolation and characterization of Dobrava hantavirus carried by the striped field mouse (*Apodemus agrarius*) in Estonia. *J Gen Virol* 80:371–379.
12. Baek LJ, *et al.* (2006) Soochong virus: A genetically distinct hantavirus isolated from *Apodemus peninsulae* in Korea. *J Med Virol* 78:290–297.
13. Duchin JS, *et al.* (1994) Hantavirus pulmonary syndrome: A clinical description of 17 patients with a newly recognized disease. *N Engl J Med* 330:949–955.
14. Nichol ST, *et al.* (1993) Genetic identification of a hantavirus associated with an outbreak of acute respiratory illness. *Science* 262:914–917.
15. Plyusnin A, Vapalahti O, Vaheri A (1996) Hantaviruses: Genome structure, expression and evolution. *J Gen Virol* 77:2677–2687.
16. Hughes AL, Friedman R (2000) Evolutionary diversification of protein-coding genes of hantaviruses. *Mol Biol Evol* 17:1558–1568.
17. Carey DE, Reuben R, Panicker KN, Shope RE, Myers RM (1971) Thottapalayam virus: A presumptive arbovirus isolated from a shrew in India. *Indian J Med Res* 59:1758–1760.
18. Zeller HG, *et al.* (1989) Electron microscopic and antigenic studies of uncharacterized viruses. II. Evidence suggesting the placement of viruses in the family *Bunyaviridae*. *Arch Virol* 108:211–227.
19. Song J-W, Baek LJ, Schmaljohn CS, Yanagihara R (2007) Thottapalayam virus: A prototype shrewborne hantavirus. *Emerg Infect Dis* 13:980–985.
20. Yadav PD, Vincent MJ, Nichol ST (2007) Thottapalayam virus is genetically distant to the rodent-borne hantaviruses, consistent with its isolation from the Asian house shrew (*Suncus murinus*). *Virol J* 4:80.
21. Song J-W, *et al.* (2007) Newfound hantavirus in Chinese mole shrew, Vietnam. *Emerg Infect Dis* 13:1784–1787.
22. Song J-W, *et al.* (2007) Seewis virus, a genetically distinct hantavirus in the Eurasian common shrew (*Sorex araneus*). *Virol J* 4:114.
23. Arai S, *et al.* (2007) Hantavirus in northern short-tailed shrew, United States. *Emerg Infect Dis* 13:1420–1423.
24. Arai S, *et al.* (2008) Phylogenetically distinct hantaviruses in the masked shrew (*Sorex cinereus*) and dusky shrew (*Sorex monticolus*) in the United States. *Am J Trop Med Hyg* 78:348–351.
25. Tkachenko EA, *et al.* (1983) Potential reservoir and vectors of haemorrhagic fever with renal syndrome (HFRS) in the U.S.S.R. *Ann Soc Belg Med Trop* 63:267–269.
26. Clement J, *et al.* (1994) in *Virus Infections of Rodents and Lagomorphs*, ed Horzinek MC (Elsevier Science BV, Amsterdam), pp 295–316.
27. Gavrilovskaya IN, *et al.* (1983) Features of circulation of hemorrhagic fever with renal syndrome (HFRS) virus among small mammals in the European U.S.S.R. *Arch Virol* 75:313–316.
28. Gligic A, *et al.* (1992) Hemorrhagic fever with renal syndrome in Yugoslavia: Epidemiologic and epizootiologic features of a nationwide outbreak in 1989. *Eur J Epidemiol* 8:816–825.
29. Ishii N (1993) Size and distribution of home ranges of the Japanese shrew-mole *Urotrichus talpoides*. *J Mamm Soc Jpn* 18:87–98.
30. Yokohata Y (2005) A brief review of the biology on moles in Japan. *Mammal Study* 30:S25–S30.
31. Shinohara A, Campbell KL, Suzuki H (2003) Molecular phylogenetic relationships of moles, shrew moles, and desmans from the new and old worlds. *Mol Phylogenet Evol* 27:247–258.
32. Shinohara A, Campbell KL, Suzuki H (2005) An evolutionary view on the Japanese talpids based on nucleotide sequences. *Mammal Study* 30:S19–S24.
33. Kawada S, Obara Y (1999) Reconsideration of the karyological relationship between two Japanese species of shrew-moles, *Dymecodon pilirostris* and *Urotrichus talpoides*. *Zoolog Sci* 16:167–174.
34. Harada M, Ando A, Tsuchiya K, Koyasu K (2001) Geographic variation in chromosomes of the greater Japanese shrew-mole, *Urotrichus talpoides* (Mammalia: Insectivora) *Zoolog Sci* 18:433–442.
35. Okumura M, *et al.* (2007) Development of serological assays for Thottapalayam virus, an insectivore-borne hantavirus. *Clin Vaccine Immunol* 14:173–181.
36. Klempa B, *et al.* (2007) Novel hantavirus sequences in shrew, Guinea. *Emerg Infect Dis* 13:520–552.
37. Kariwa H, *et al.* (1999) Genetic diversities of hantaviruses among rodents in Hokkaido, Japan and Far East Russia. *Virus Res* 59:219–228.
38. Zou Y, *et al.* (2008) Isolation and genetic characterization of hantaviruses carried by Microtus voles in China. *J Med Virol* 80:680–688.
39. Zou Y, *et al.* (2008) Genetic analysis of hantaviruses carried by reed voles Microtus fortis in China. *Virus Res* 137:122–128 .
40. Plyusnina A, *et al.* (2008) Genetic analysis of hantaviruses carried by *Myodes* and *Microtus* rodents in Buryatia. *Virol J* 5:4
41. Vapalahti O, *et al.* (1999) Isolation and characterization of a hantavirus from *Lemmus sibiricus*: Evidence for host switch during hantavirus evolution. *J Virol* 73:5586–5592.
42. Thompson JD, Higgins DG, Gibson TJ (1994) CLUSTAL W: Improving the sensitivity of progressive multiple sequence alignment through sequence weighting, position-specific gap penalties and weight matrix choice. *Nucl Acids Res* 22:4673–4680.
43. Ronquist F, Huelsenbeck JP (2003) MrBayes 3: Bayesian phylogenetic inference under mixed models. *Bioinformatics* 19:1572–1574.
44. Posada D, Crandall KA (1998) MODELTEST: Testing the model of DNA substitution. *Bioinformatics* 14:817–818.
45. Swofford DL (2003) PAUP*. Phylogenetic analysis using parsimony (*and other methods). Version 4 (Sinauer Associates, Sunderland, Massachusetts).
46. Whelan S, Goldman N (2001) A general empirical model of protein evolution derived from multiple protein families using a maximum-likelihood approach. *Mol Biol Evol* 18:691–699.
47. Combet C, Blanchet C, Geourjon C, Deléage G (2000) NPS@: Network Protein Sequence Analysis. *Trends Biochem Sci* 25:147–150.
48. King RD, Sternberg MJ (1996) Identification and application of the concepts important for accurate and reliable protein secondary structure prediction. *Protein Sci* 5:2298–2310.
49. Guermeur Y, Geourjon C, Gallinari P, Deléage G (1999) Improved performance in protein secondary structure prediction by inhomogeneous score combination. *Bioinformatics* 15:413–421.
50. Rost B, Sander C (1993) Prediction of protein secondary structure at better than 70% accuracy. *J Mol Biol* 232:584–599.
51. Frishman D, Argos P (1996) Incorporation of non-local interactions in protein secondary structure prediction from the amino acid sequence. *Protein Eng* 9:133–142.
52. Garnier J, Gibrat J-F, Robson B (1996) GOR method for predicting protein secondary structure from amino acid sequence. *Methods Enzymol* 266:540–553.
53. Levin JM, B. Robson B, Garnier J (1986) SIMPA96: An algorithm for secondary structure determination in proteins based on sequence similarity. *FEBS Lett* 205:303–308.
54. Geourjon C, Deléage G (1995) SOPMA: Significant improvements in protein secondary structure prediction by consensus prediction from multiple alignments. *Comput Appl Biosci* 11:681–684.
55. Irwin DM, Kocher TD, Wilson AC (1991) Evolution of the cytochrome b gene of mammals. *J Mol Evol* 32:128–144.

JOURNAL OF VIROLOGY, Jan. 2010, p. 459–474 Vol. 84, No. 1
0022-538X/10/$12.00 doi:10.1128/JVI.01226-09

Extensive Host Sharing of Central European Tula Virus▽

Jonas Schmidt-Chanasit,[1]† Sandra Essbauer,[2]† Rasa Petraityte,[3] Kumiko Yoshimatsu,[4] Kirsten Tackmann,[5] Franz J. Conraths,[5] Kestutis Sasnauskas,[3] Jiro Arikawa,[4] Astrid Thomas,[2] Martin Pfeffer,[2] Jerrold J. Scharninghausen,[6] Wolf Splettstoesser,[2] Matthias Wenk,[7] Gerald Heckel,[8] and Rainer G. Ulrich[9]*

Bernhard Nocht Institute for Tropical Medicine, Hamburg, Germany[1]; Bundeswehr Institute of Microbiology, Munich, Germany[2]; Institute of Biotechnology, Vilnius, Lithuania[3]; Institute for Animal Experimentation, Hokkaido University, Sapporo, Japan[4]; Friedrich-Loeffler-Institut, Federal Research Institute for Animal Health, Institute for Epidemiology, Wusterhausen, Germany[5]; Department of Global Health, College of Public Health, University of South Florida, Tampa, Florida[6]; Landesforstanstalt Eberswalde, Eberswalde, Germany[7]; Computational and Molecular Population Genetics (CMPG), Institute of Ecology and Evolution, University of Bern, Bern, and Swiss Institute of Bioinformatics, Lausanne, Switzerland[8]; and Friedrich-Loeffler-Institut, Federal Research Institute for Animal Health, Institute for Novel and Emerging Infectious Diseases, Greifswald-Insel Riems, Germany[9]

Received 14 June 2009/Accepted 16 October 2009

To examine the host association of Tula virus (TULV), a hantavirus present in large parts of Europe, we investigated a total of 791 rodents representing 469 *Microtus arvalis* and 322 *Microtus agrestis* animals from northeast, northwest, and southeast Germany, including geographical regions with sympatric occurrence of both vole species, for the presence of TULV infections. Based on serological investigation, reverse transcriptase PCR, and subsequent sequence analysis of partial small (S) and medium (M) segments, we herein show that TULV is carried not only by its commonly known host *M. arvalis* but also frequently by *M. agrestis* in different regions of Germany for a prolonged time period. At one trapping site, TULV was exclusively detected in *M. agrestis*, suggesting an isolated transmission cycle in this rodent reservoir separate from spillover infections of TULV-carrying *M. arvalis*. Phylogenetic analysis of the S and M segment sequences demonstrated geographical clustering of the TULV sequences irrespective of the host, *M. arvalis* or *M. agrestis*. The novel TULV lineages from northeast, northwest, and southeast Germany described here are clearly separated from each other and from other German, European, or Asian lineages, suggesting their stable geographical localization and fast sequence evolution. In conclusion, these results demonstrate that TULV represents a promiscuous hantavirus with a large panel of susceptible hosts. In addition, this may suggest an alternative evolution mode, other than a strict coevolution, for this virus in its *Microtus* hosts, which should be proven in further large-scale investigations on sympatric *Microtus* hosts.

Hantaviruses (genus *Hantavirus*, family *Bunyaviridae*) are characterized by a tripartite RNA genome of negative polarity. The small (S) genome segment of about 1.7 kb encodes the nucleocapsid (N) protein that is associated as a multimer with the viral RNA genome. The medium (M) segment of about 3.6 kb encodes a glycoprotein precursor that is cotranslationally cleaved at a highly conserved WAASA motif into the G1 and G2 envelope glycoproteins. These proteins form oligomers which mediate the interaction of the virus with the cellular receptor. The large (L) segment of about 6.5 kb encodes the RNA-dependent RNA polymerase that functions as transcriptase and replicase (for a review, see reference 57).

In general, hantaviruses are harbored by persistently infected rodent reservoir hosts which shed the hantaviruses by urine, feces, and saliva. Therefore, the major route of transmission to humans is by inhalation of aerosols originating from virus-contaminated urine or feces (for a review, see reference 58). The high stability of hantaviruses in nature allows indirect transmission and underlines the importance of environmental factors on the frequency of transmission (31). An alternative route of virus transmission to humans is by rodent bites (10). Human-to-human transmission has exclusively been observed for the South American Andes virus (42).

The congruent phylogenetic affinities of hantaviruses and their corresponding reservoir hosts are currently explained by a virus-host coevolution hypothesis (46). According to this theory, each hantavirus species is associated with a single rodent species or a closely related species of the same genus. This close host/pathogen association is also believed to determine viral properties and therefore the pathogenicity in humans (73).

Tula virus (TULV) has primarily been identified in the European common voles *Microtus arvalis* and *Microtus rossiaemeridionalis* collected from the Tula area of Russia, located 200 kilometers south of Moscow, and in *M. arvalis* in western Slovakia, near the town of Malacky (43, 61). Subsequently, TULV has been detected in other related rodent species of the subfamily Arvicolinae, i.e., *M. agrestis*, *Microtus gregalis*, *Micro-*

* Corresponding author. Mailing address: Friedrich-Loeffler-Institut, Federal Research Institute for Animal Health, OIE Collaborating Centre for Zoonoses in Europe, Institute for Novel and Emerging Infectious Diseases, Südufer 10, D-17493 Greifswald-Insel Riems, Germany. Phone: 49-38351-7159. Fax: 49-38351-7192. E-mail: rainer.ulrich@fli.bund.de.
† These authors contributed equally to this article.
▽ Published ahead of print on 4 November 2009.

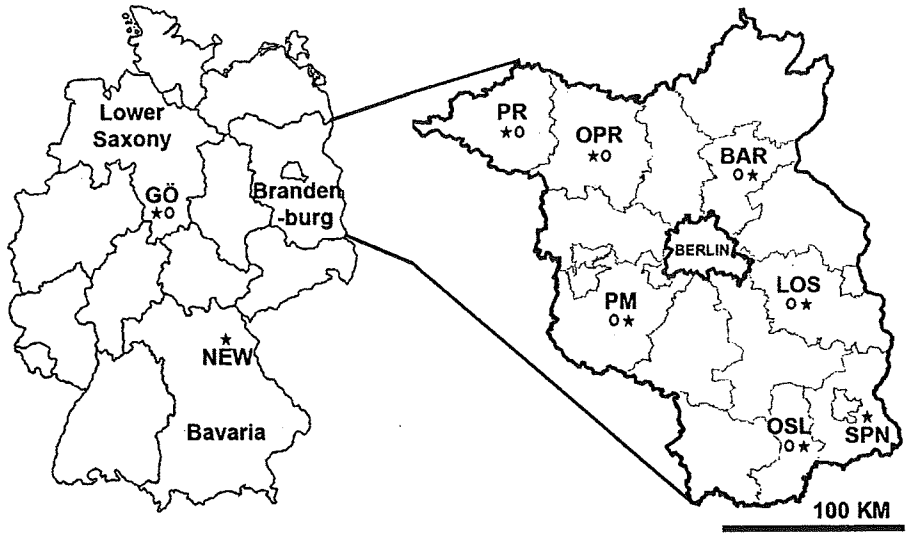

FIG. 1. Geographical localization of the trapping sites in six districts in Brandenburg, northeast Germany, one location in Lower Saxony, northwest Germany, and one location in Bavaria, southeast Germany. In addition, the localization of trapping sites of *M. arvalis*, where TULV sequences were detected in a previous study, is given (32). GÖ, Göttingen; NEW, Neustadt/Waldnaab; PR, Prignitz; OPR, Ostprignitz-Ruppin; BAR, Barnim; PM, Potsdam-Mittelmark; LOS, Oder-Spree; OSL, Oberspreewald-Lausitz; SPN, Spree-Neisse.

tus (*Pitymys*) *subterraneus*, and *Lagurus lagurus* (56, 65; A. E. Dekonenko and V. V. Yakimenko, unpublished data) (GenBank accession number AF442620-21). TULV-positive rodents have been detected in a number of European countries, such as Russia, Slovakia, Croatia, the Czech Republic, Austria, Poland, Belgium, Germany, France, Hungary, The Netherlands, and Slovenia (4, 6, 21, 30, 32, 35, 43, 44, 47, 51, 56, 61, 65, 66).

Hantaviruses associated with the genus *Microtus* (subfamily Arvicolinae) have currently only rarely been associated with human disease. Although the North American viruses Prospect Hill virus (PHV), isolated from the meadow vole *Microtus pennsylvanicus* (38), Bloodland Lake virus, detected in the prairie vole *Microtus ochrogaster* (22), and Isla Vista virus (ISLAV), detected in the Californian vole *Microtus californicus* (64), have not been shown to cause significant disease in humans, experimental infections of nonhuman primates with PHV caused an acute nephropathy (74). Similarly, the Eurasian hantavirus species Khabarovsk virus hosted by the reed vole *Microtus fortis* (23) and TULV are believed to have no or low pathogenicity for humans. However, a few human TULV infections have been reported, with two case reports about potential TULV-induced disease in humans (32, 59, 70, 71). This low frequency in the detection of human TULV infections might be explained by its low pathogenic potential (36); however, human TULV infections might have been overlooked because their differentiation from infections with the TULV-cross-reactive Puumala virus (PUUV) would require a neutralization assay (70).

Here we report on data from the first longitudinal monitoring study of TULV in Europe, with samples collected over a period of 12 years. These investigations showed the sympatric occurrence of TULV in *M. arvalis* and *M. agrestis* at several localities and in different years. Phylogenetic analysis of the TULV sequences demonstrates a geographical clustering which is independent from the rodent reservoir species. This provides strong evidence for isolated replication and transmission cycles of TULV in both species, along with frequent multiple spillover infections of TULV between *M. arvalis* and *M. agrestis* populations.

MATERIALS AND METHODS

Rodents. Between 1994 and 2005, *Microtus* rodents were trapped in six districts of the Federal State of Brandenburg, northeast Germany, and in 2005, they were trapped at one site (Sennickerode [SEN]) in the district Göttingen (GÖ) in the Federal State of Lower Saxony, northwest Germany. Additional rodents were trapped between 1994 and 1997 at four different military training areas, including Grafenwöhr, district Neustadt/Waldnaab (NEW), located in the Federal State of Bavaria, southeast Germany (Fig. 1 and Tables 1 and 2). Captured rodents were weighed and measured, and their gender and species were identified. For serological analysis, transudate samples were collected from the thoracic cavity of rodents from Brandenburg. From rodents trapped from 1994 to 1997 in Brandenburg or Bavaria, only brain or kidney samples were available. From rodents trapped from 2002 to 2005 in Brandenburg and Lower Saxony, lung, heart, liver, spleen, kidney, and brain samples were collected. Tissue samples were stored at −20°C until processing with reverse transcriptase PCR (RT-PCR). Morphological species determination of TULV RT-PCR-positive animals was confirmed by using a PCR specific for the mitochondrial cytochrome *b* gene (11).

Serological screening. To detect hantavirus-specific immunoglobulin G (IgG) antibodies, rodent transudates were screened by using enzyme-linked immunosorbent assays (ELISA) and Western blot (WB) tests based on *Saccharomyces cerevisiae*-expressed His-tagged N proteins of PUUV strain Vranica/Hällnäs (9, 50) and TULV strain Moravia (44; M. Mertens, R. Petraityte, K. Sasnauskas, R. Friedrich, and R. G. Ulrich, unpublished data). Assays were performed as described previously (11). Selected seroreactive samples were confirmed by focus reduction neutralization test analysis, according to protocols described earlier (3).

Statistical analysis. Potential associations between gender and age, using body mass as a proxy, and seropositivity to hantavirus in voles were analyzed using the chi-square test, Mann-Whitney test, or Fisher exact test included in the software package SPSS (SPSS version 12.0.1, SPSS Inc., Chicago, IL) and by Win Episcope 2.0 (69).

RT-PCR and sequencing. RNA from all animals from Lower Saxony and Bavaria and from TULV-seroreactive animals from Brandenburg was extracted

TABLE 1. Serological reactivity of transudates from *Microtus arvalis* and *M. agrestis* trapped during 1994 to 1997 at different trapping sites in Brandenburg

Species	Trapping year	No. of trapped rodents/no. of serologically reactive transudates of these rodents (%)										
		OPR trapping sites					PR trapping sites					Total
		Kyritz	Segeletz	Nackel	Breddin	Subtotal	Bendelin	Granzow	Glöwen	Schönhagen	Subtotal	
M. arvalis	1994	12/1	0	0	0	12/1 (8)	34/2	22/4	0	0	58/6[b] (10)	70/7 (10)[b]
	1995	1/0	42/8	7/1	0	53/9[a] (17)	15/2	61/12	35/17	31/8	142/39 (27)	195/48 (25)
	1996	34/3	0	0	10/2	44/5 (11)	16/3	0	2	6/1	24/4 (17)	68/9 (13)
	1997	1/0	0	0	0	1/0	10/3	0	4/0	29/3	43/6 (14)	44/6 (14)
	Total	48/4	42/8	7/1	10/2	110/15[a] (14)	75/10	83/16	41/17	66/12	267/55[b] (21)	377/70[a,b] (19)
M. agrestis	1994	0	0	0	0	0	11/3	24/1	0	0	35/4 (11)	35/4 (11)
	1995	0	0	1/1	0	1/1 (100)	11/0	0	0	0	11/0	12/1 (8)
	1996	1/1	0	2/0	0	3/1 (33)	0	0	0	0	0	3/1 (33)
	1997	0	0	0	0	0	0	0	0	0	0	0
	Total	1/1	0	3/1	0	4/2 (50)	22/3	24/1	0	0	46/4 (9)	50/6 (12)

[a] Total numbers contain three additional seronegative *M. arvalis* rodents trapped in 1995 in Netzeband, Germany.
[b] Total numbers contain two additional seronegative *M. arvalis* rodents trapped in 1994 in Perleberg, Germany.

from brain, heart, or lung tissue samples using commercial kits (11). Single-step and nested RT-PCRs using primers targeting the S segment were performed with primer pairs DOBV-M6/DOBV-M8, PUUV 342/cPUUV 1102, SNMa1/MaS4C, and S1/S10PC and nested primers PUUV390/cPUUV721 as described previously (11, 55, 61, 62). The partial M segment was amplified using primers C1, 5′-CC CCCTGATTGTCCTGGTGTAG-3′, and C2, 5′-CCAACTCCTGAACCCCAT GC-3′ (corresponding to nucleotides [nt] 2369 to 2390 and nt 3011 to 3031 of PUUV strain Sotkamo, GenBank accession number X61034). Direct sequencing of the purified PCR products was done using the S and M segment-specific primers described above. GenBank accession numbers of the novel TULV sequences are shown (see Table 4).

Sequence comparison and phylogenetic analysis. Nucleotide sequences were aligned in BioEdit 5.0.9 (17) and revised manually. Phylogenetic relationships among nucleotide sequences were reconstructed with neighbor-joining (NJ) (54) and maximum likelihood (ML) algorithms implemented in PAUP* 4.0b (67) using two PUUV strains as the outgroup and 5,000 bootstrap replicates. Hierarchical likelihood ratio tests and the Akaike information criterion (1) implemented in Modeltest 3.06 (48) were used to estimate the most suitable model of nucleotide substitution. The best substitution model for the S segment was the general time-reversible (GTR) model with gamma distribution (68) with the following parameters: substitution rate matrix, A ↔ C, 4.1689; A ↔ G, 14.7655; A ↔ T, 3.1028; C ↔ G, 0.6093; C ↔ T, 22.7757; and G ↔ T, 1.0000; gamma distribution shape parameter, 0.1931. The base frequencies were estimated as follows: A, 0.3318; C, 0.2114; G, 0.1966; and T, 0.2602. For the M segment, the best substitution model was the GTR model with invariable sites and gamma distribution (52). The following parameters for the model were estimated: substitution rate matrix, A ↔ C, 4.8675; A ↔ G, 16.5929; A ↔ T, 1.5562; C ↔ G, 4.9664; C ↔ T, 36.3308; and G ↔ T, 1.0000; gamma distribution shape parameter, 0.5635; proportion of invariable sites, 0.4103; base frequencies, A, 0.3568; C, 0.1519; G, 0.1657; and T, 0.3256.

Estimates of evolutionary raw divergence and standard error estimates (500 bootstrap replicates) over sequence pairs between groups were obtained by pairwise analysis, as supplied by MEGA4 (37). Codon positions included were first plus second plus third plus noncoding. All positions containing gaps and missing data were eliminated from the data set (complete deletion option).

Morphological species designations of TULV-positive rodents were verified by performing BLAST searches of the novel cytochrome *b* sequences with sequences available in GenBank (http://www.ncbi.nlm.nih.gov). The cytochrome *b* sequences of TULV-positive *M. agrestis* and *M. arvalis* were further compared to those from larger surveys of genetic diversity in these rodents across Germany and neighboring countries (14, 19, 25). Representative sequences from all evolutionary lineages present in Europe in *M. arvalis* and *M. agrestis* were obtained from GenBank. Technical details on phylogenetic reconstructions from cytochrome *b* are given elsewhere (15, 16, 19).

RESULTS

Rodent trapping in the longitudinal study and cytochrome *b* analysis of *Microtus* spp. Between 1994 and 1997, a total of 427 *Microtus* rodents, with 377 *M. arvalis* rodents, 115 male and 262 female, and 50 *M. agrestis* rodents, 24 male and 26 female, were trapped at 10 sites in two different districts (Ostprignitz-Rup-

TABLE 2. Serological reactivity of transudates from *Microtus arvalis* and *M. agrestis* trapped during 2002 to 2005 at different trapping sites in Brandenburg[a]

Species	Trapping year	No. of trapped rodents/no. of serologically reactive transudates of these rodents (%)						
		BAR trapping sites			LOS trapping site Wendisch	PM trapping site MRZ	OSL trapping site Altdöbern	Total
		Bernau	EBE	Subtotal				
M. arvalis	2002	47/0	1/0	48	0	0	1/0	49
	2003	0	0	0	0	0	0	0
	2004	0	1/1	1/1 (100)	0	0	6/0	7/1 (14)
	2005	0	0	0	9/0	1/0	0	10
	Total	47/0	2/1	49/1 (2)	9/0	1/0	7/0	66/1 (2)
M. agrestis	2002	3/0	14/4	17/4 (24)	7/0	45/3 (7)	4/0	73/7 (10)
	2003	15/0	16/0	31/0	8/0	21/1 (5)	0	60/1 (2)
	2004	1/0	13/0	14/0	21/0	15/1 (7)	2/0	52/1 (2)
	2005	0	26/1	26/1 (4)	13/0	36/1 (3)	10/0	85/2 (2)
	Total	19/0	69/5	88/5 (6)	49/0	117/6 (5)	16/0	270/11 (4)

[a] EBE, Eberswalde; MRZ, Marzehns.

pin [OPR] and Prignitz [PR]) in the Federal State of Brandenburg, northeast Germany (Fig. 1 and Tables 1 and 2). In addition, a total of 336 *Microtus* rodents, including 58 male and 8 female *M. arvalis* rodents and 122 male and 148 female *M. agrestis* rodents, were trapped at five sites in four other districts (Barnim [BAR], Oder-Spree [LOS], Potsdam-Mittelmark [PM], and Oberspreewald-Lausitz [OSL]) in the Federal State of Brandenburg between 2002 and 2005 (Fig. 1 and Tables 1 and 2). Altogether, *M. arvalis* and *M. agrestis* were trapped at nine sites in Brandenburg, with a sympatric occurrence of *M. arvalis* and *M. agrestis* in the same year of trapping (Tables 1 and 2). In 2005, 16 *M. arvalis* rodents, 5 female and 11 male, and 2 male *M. agrestis* rodents were trapped at a single site in Lower Saxony (SEN, GÖ) (Fig. 1). From 1994 to 1997, 10 *M. arvalis* rodents were trapped at one site in the military training area Grafenwöhr (NEW) in Bavaria (Fig. 1).

Sequencing of cytochrome *b* genes of selected *M. arvalis* and *M. agrestis* rodents from Brandenburg and Lower Saxony confirmed the morphological species determination (see Table 4). Phylogenetic reconstructions of rodent host relationships based on the mitochondrial cytochrome *b* gene showed a clear differentiation between *M. arvalis* and *M. agrestis* and an additional substructure among voles from different European regions (Fig. 2). All *M. arvalis* rodents from the German study sites belonged to the Central evolutionary lineage of this species, and all *M. agrestis* rodents from these sites belonged to the Western lineage. This is in agreement with the general distribution of these lineages, as determined in larger surveys of the two species (14, 19, 25).

In total, 791 *Microtus* rodents were trapped at 17 sites located in eight different districts in northeast, southeast, and northwest Germany.

Serological analysis of rodent transudates. An initial IgG ELISA screening using recombinant PUUV N protein as the antigen revealed a total of 35 seroreactive animals out of 763 animals (4.6%) from Brandenburg (data not shown). For 28 out of 35 samples (80%), the immunoreactivity was confirmed by a corresponding PUUV WB test (data not shown). In parallel, all transudate samples were tested by an IgG ELISA using recombinant TULV N antigen (Tables 1 and 2). Using this test format, TULV-reactive antibodies were detected in 71 of 443 *M. arvalis* transudates (16%) and 17 of 320 *M. agrestis* transudates (5.3%), demonstrating a much higher level of sensitivity for the TULV ELISA than that for the PUUV test. For 25 out of 30 TULV- and PUUV-IgG ELISA-reactive samples (83%), the endpoint titer was higher in the TULV assay (Table 3). For the majority (75 of 88; 88%) of transudates, the TULV ELISA reactivity was confirmed in a TULV WB test (data not shown). The *M. arvalis*-seroreactive samples originated from both male (31 of 173; 17.3%) and female (40 of 270; 14.8%) animals. In contrast, seroreactivity in *M. agrestis* transudates demonstrated a strong gender bias, with 15 out of 146 male (10.3%) but only 2 out of 174 female (1.1%) animals being seroreactive, which proved to be statistically significant (chi-square test, P of <0.001; odds ratio, 8.9; Fisher's exact test, P of <0.001). In contrast, the differences in the TULV seroprevalence between the genders in *M. arvalis* were not statistically significant (chi-square test, P of 0.416; odds ratio, 1.210; Fisher's exact test, P of 0.513). The body mass of *M. agrestis*, which was used as a proxy for the age of the animals, was found to be positively associated with the seropositivity (Mann-Whitney test, P of 0.0058), whereas this was not statistically significant for *M. arvalis* (Mann-Whitney test, P of 0.0703).

To prove the validity of the ELISA and WB tests, five *M. arvalis* and four *M. agrestis* transudates were tested by focus reduction neutralization assays using TULV, PUUV, Dobrava virus, and Saaremaa virus. For all nine transudates, the highest endpoint titer was observed for TULV, confirming TULV infections in both rodent species (Table 3).

The serological investigations demonstrated the presence of TULV-reactive antibodies in both *M. arvalis* and *M. agrestis*, with differences depending on the species, the trapping site, the gender, and the age of the rodents.

RT-PCR analysis of tissue samples. For 19 out of 20 seroreactive animals from Brandenburg whose brain, heart, or lung tissue samples were available, the investigations with S segment-specific RT-PCR or nested RT-PCR revealed specific amplification products (Table 4). The positive samples originated from four male and three female *M. arvalis* rodents and 11 male and one female *M. agrestis* rodents. One sample (Mu/04/151) from a seropositive female *M. agrestis* rodent tested negative in all RT-PCRs used. Sequencing of the amplification products resulted in the identification of TULV sequences in samples from both *M. arvalis* and *M. agrestis* (Table 4). As expected for RT-PCR investigations of lung samples, sequence information for all tested animals was obtained, with the majority of sequences being about 700 nt in size. Interestingly, the nested RT-PCR approach was successful for all tested brain samples from seven animals when no other tissue samples were available. In addition, for four out of five investigated heart samples, partial S segment-specific sequences were obtained (Table 4).

Screening of lung samples from all 16 *M. arvalis* and 2 *M. agrestis* rodents from Lower Saxony (district GÖ, site SEN) by S segment-specific RT-PCR revealed six positive *M. arvalis* results from one female and five male animals. In addition, one male *M. agrestis* animal was PCR positive (Table 4). Larger PCR fragments (from 1,347 nt up to 1,708 nt in length) (Table 4) could be derived from all positive samples.

Out of the 10 *M. arvalis* animals from Bavaria (Grafenwöhr, NEW), two kidney samples allowed the amplification of TULV S segment sequences of 334 and 1,832 nt in length (Table 4).

In addition to the S segment sequences, M segment sequences were obtained by RT-PCR amplification of the region spanning nt 2369 to 3031 (numbering according to PUUV strain Sotkamo, GenBank accession number X61034) for four *M. arvalis* animals, three from Lower Saxony and one from Brandenburg, and five *M. agrestis* animals from Brandenburg.

In summary, TULV S and M segment sequences were detected in both *M. arvalis* and *M. agrestis*.

Phylogenetic analyses of TULV sequences. In contrast to the rodent data, phylogenetic analyses of both the S and M segments revealed very strong geographical but no host-specific affinities of TULV sequences. Phylogenetic trees reconstructed from 80 sequences of a 333-nt-long S segment (nt positions 355 to 686 in TULV strain Lodz-2, GenBank accession number AF063897) demonstrated that the novel TULV sequences from northwest and southwest Brandenburg and Lower Saxony (lineages Germany I and II) were

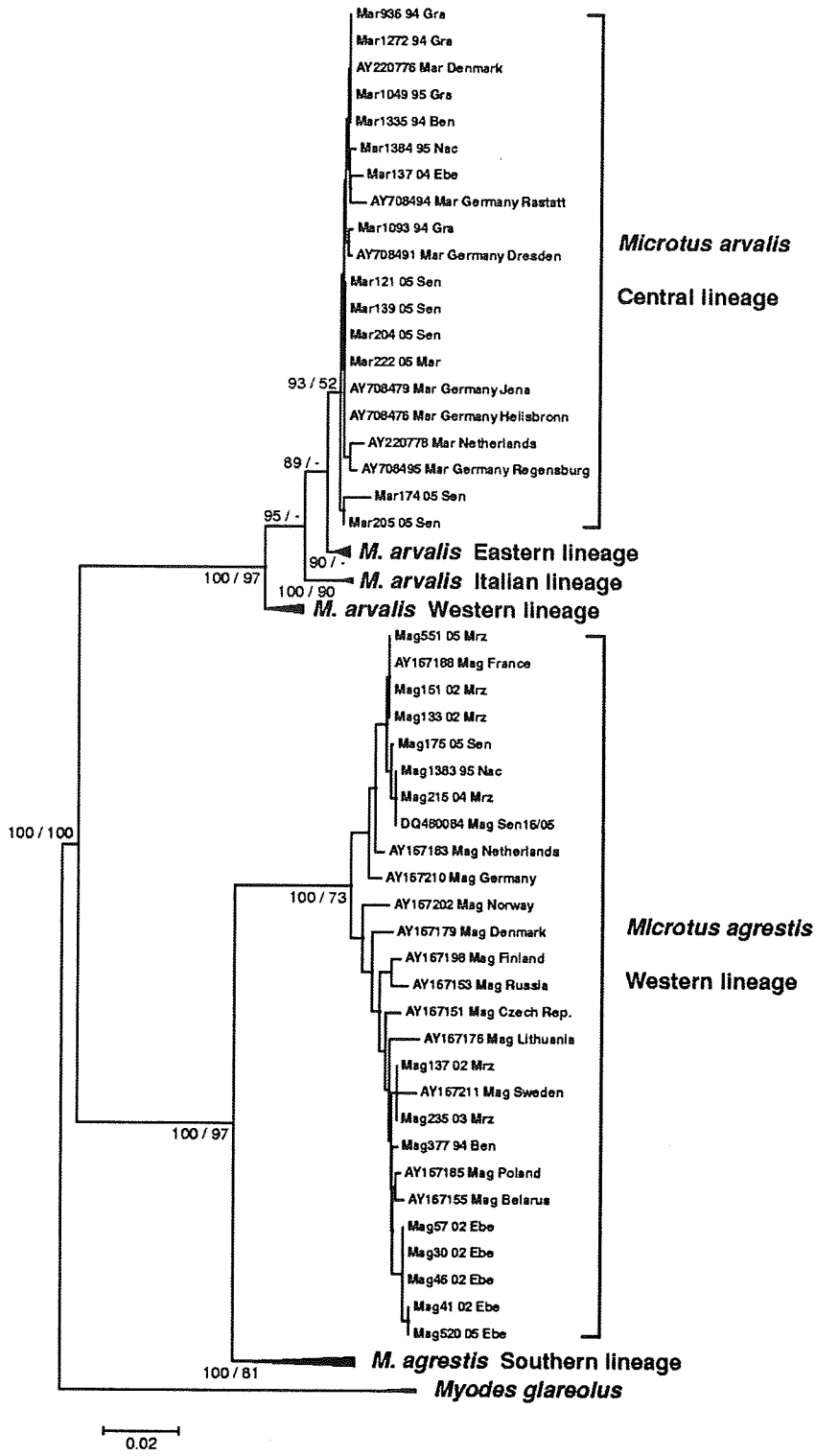

FIG. 2. NJ tree reconstructed from cytochrome *b* DNA sequence data of TULV-positive *M. arvalis* and *M. agrestis*, with two sequences from the closely related *Myodes glareolus* (host of PUUV) as the outgroup. All new sequences from this study (labels beginning with Mar or Mag) belong to the Central lineage in *M. arvalis* (8, 14, 19) or to the Western lineage in *M. agrestis* (25, 26). The robustness of nodes in phylogenetic trees based on NJ and ML algorithms was tested with 5,000 bootstrap replicates each. Only bootstrap values of >50% for main branches connecting major evolutionary lineages are displayed for NJ (before slash) and ML (after slash). Consistent with larger surveys of *M. arvalis* and *M. agrestis*, relationships among sequences within evolutionary lineages are unresolved and phylogenetically unstable due to insufficient variation in cytochrome *b* (for an example, see reference 14). The accession numbers of cytochrome *b* sequences used for comparison are given in Table 8.

TABLE 3. Immunoreactivity of transudates from *Microtus arvalis* and *M. agrestis* in TULV and PUUV IgG ELISA and focus reduction neutralization tests

Rodent no.[a]	Species	Endpoint titer results[b]					
		IgG ELISA		FRNT			
		TULV	PUUV	TULV	PUUV	SAAV	DOBV
Mar1738_95_Gra	*M. arvalis*	**200**	<200	**160**	40	<40	<40
Mar1782_95_Glo	*M. arvalis*	**400**	200	**320**	<40	<40	<40
Mar1831_95_Glo	*M. arvalis*	200	200	**160**	80	40	80
Mar2053_95_Scho	*M. arvalis*	400	400	**320**	40	40	<40
Mar2057_95_Scho	*M. arvalis*	**800**	200	**320**	80	40	<40
Mag377_94_Ben	*M. agrestis*	**3,200**	800	**80**	<40	<40	<40
Mag544_94_Gra	*M. agrestis*	**800**	200	**40**	<40	<40	<40
Mag1383_95_Nac	*M. agrestis*	ND	400	**>1,280**	40	<40	<40
Mag30_02_Ebe	*M. agrestis*	**1,600**	800	**640**	160	<40	<40
Positive control (anti-PUU B.N)	Human	ND	ND	<40	160	<40	<40
Negative control (NHS-007)	Human	ND	ND	<40	<40	<40	<40

[a] The rodent numbers reflect the species (Mar, *M. arvalis*; Mag, *M. agrestis*), the number of the rodent, trapping year, and trapping site in the different districts (Glo, Glöwen, Prignitz; Scho, Schönhagen, Prignitz; Gra, Granzow, Prignitz; Nac, Nackel, Ostprignitz-Ruppin; Ebe, Eberswalde, Barnim; Ben, Bendelin, Prignitz); for geographical localization of trapping sites, see Fig. 1.

[b] The highest endpoint titer for each sample is highlighted in boldface. FRNT, focus reduction neutralization test; SAAV, Saaremaa virus; DOBV, Dobrava virus; ND, not determined.

clearly separated from other German lineages originating from Bavaria, southeast Germany (Germany IV), and southeast Brandenburg (Germany III) (Fig. 3A). A more detailed evaluation of clusters Germany I and II showed a geographical clustering of these sequences irrespective of the rodent host species (Fig. 3B). The sublineage IA from the trapping sites Granzow and Bendelin (district PR) and Nackel (district OPR) was predominantly detected in *M. arvalis* but also in one *M. agrestis* animal. A similar pattern was observed for TULV infections in *Microtus* from SEN (district GÖ; lineage Germany II). In Eberswalde (EBE) (district BAR; sublineage IB), TULV infections were found mostly in *M. agrestis* but also in one *M. arvalis* animal. At the trapping site Marzehns (MRZ) (district PM) in southwest Brandenburg, exclusively TULV-infected *M. agrestis* animals were found between 2002 and 2005, but no TULV-infected *M. arvalis* animal was found (Tables 1, 2, and 4).

The analysis of M segment nucleotide sequences (nt positions 2390 to 3010) (Fig. 4) and corresponding amino acid sequences (amino acid [aa] positions 780 to 985 of GPC in the G2 part) supported the patterns detected in the S segment (data not shown). The novel sequences from Germany were clearly distinct from all M segment sequences published so far. Again, the *M. arvalis*-associated sequence from Mar137_04_EBE (district BAR) grouped together with four *M. agrestis*-associated TULV sequences in the cluster Germany I. Similarly, the Germany II clade consisted of TULV M sequences associated with *M. arvalis* and *M. agrestis*.

Therefore, phylogenetic analysis revealed a geographical, but not host-specific, clustering of TULV S and M segment sequences from two different *Microtus* species. In addition, these investigations showed for the first time that TULV is (probably) able to establish an isolated transmission cycle in *M. agrestis*.

Molecular analysis of S and M segment nucleotide sequences. A pairwise comparison of TULV S and M segment nucleotide sequences from animals within the clusters of TULV revealed a high level of divergence. The levels of the average nucleotide (amino acid) partial S segment sequence divergence in groups Germany I and Germany II were up to 7.2% (0.2%) and 5.4% (0.2%), respectively (Table 5). Similarly, sequences of clusters Russia I, Russia II, and Russia III showed divergence levels of 5.3 to 6.8% (0 to 2.3%). In contrast, the other clusters, including Germany III, Slovakia III/Czech Republic, Austria I and II, Poland, and Slovakia I and II, displayed lower average intercluster divergence levels of 0 to 1.9% (0 to 0.3%).

The divergence level of the S segment nucleotide sequences between the clusters from Germany was surprisingly high (about 12 to 20%) (Table 6). The divergence level of about 18% between sequences from clusters I and II and those from cluster III is particularly important, as all sequences in clusters I (districts OPR, PR, and BAR) and III (district Spree-Neisse [SPN]) and about one-half of the sequences in cluster II (districts PM and OPR) originated from closely related geographical sites in Brandenburg (Fig. 1). The nucleotide sequence divergence level of TULV sequences from other European regions also ranged from 17 to 20%. Interestingly, the amino acid sequence divergence level between sequences from clusters Germany I and II and those from cluster Germany IV was higher than the divergence levels for all other sequences from Europe.

The full-length open reading frame (ORF) of the N protein made up of 430 codons was able to be amplified from four RT-PCR-positive *Microtus* sequences from SEN (district GÖ; SEN 174, 175, 204, and 205) and one from Grafenwöhr (district NEW; AF164093). A putative second ORF encoding a hypothetical nonstructural protein, NSs, made up of 90 aa (corresponding to nt 84 to 356) was determined for these four sequences of *Microtus* from SEN and the one from Grafenwöhr. The entire N-encoding sequence in the samples from Bavaria was 84.2 to 84.6% identical at the nucleotide level and 95.3 to 95.8% identical at the amino acid level to the corresponding sequences from SEN (data not shown). For the N ORF, the nucleotide and amino acid sequences of Mar204_05_SEN, Mar205_05_SEN, and Mar174_05_SEN dif-

TABLE 4. GenBank accession numbers for TULV S and M segment sequences and cytochrome *b* sequences from *Microtus arvalis* and *M. agrestis* from Brandenburg, Lower Saxony, and Bavaria[a]

Rodent no.[b]	District	Species	Sex	Tissue type	Positive S segment result(s) for RT-PCRs[c]	Length of final fragment (nt)	GenBank accession no. for indicated sequences		
							Cytochrome *b*	S segment	M segment
Mar1335_94_Ben	PR	*M. arvalis*	M	Brain	N	287	DQ768133	EF409820	ND
Mag377_94_Ben	PR	*M. agrestis*	M	Lung	P, D	696	DQ662096	DQ662088	ND
Mar1272_94_Gra	PR	*M. arvalis*	M	Brain	N	287	DQ768138	EF409819	ND
Mar936_94_Gra	PR	*M. arvalis*	F	Brain	D, N	624	DQ768136	DQ768137	ND
Mar1093_94_Gra	PR	*M. arvalis*	M	Brain	D, N	624	DQ768134	DQ768135	ND
Mar1049_95_Gra	PR	*M. arvalis*	F	Brain	N	287	DQ768139	EF409818	ND
Mar1384_95_Nac	OPR	*M. arvalis*	F	Brain	D, N	624	DQ768131	DQ768132	ND
Mag1383_95_Nac	OPR	*M. agrestis*	M	Brain	N	287	DQ768140	EF409821	ND
Mag20_97_Grf	NEW	*M. arvalis*	ND	Kidney	S, S1	1832	ND	AF164093	ND
Mag28_97_Grf	NEW	*M. arvalis*	ND	Kidney	D	334	ND	AF164092	ND
Mag30_02_Ebe	BAR	*M. agrestis*	M	Lung	P, D	703	DQ662098	DQ662090	DQ665814
Mag41_02_Ebe	BAR	*M. agrestis*	M	Lung	P, D	703	DQ662099	DQ662091	DQ665815
Mag46_02_Ebe	BAR	*M. agrestis*	M	Lung	P, D	702	DQ662095	DQ662087	DQ665812
Mag57_02_Ebe	BAR	*M. agrestis*	M	Lung	P, D	713	DQ662100	DQ662092	DQ665813
Mag133_02_Mrz	PM	*M. agrestis*	F	Lung	P, D	696	DQ662101	DQ662093	ND
Mag137_02_Mrz	PM	*M. agrestis*	M	Heart	P, D	713	DQ662102	DQ662094	ND
Mag235_03_Mrz	PM	*M. agrestis*	M	Lung	D, N	624	DQ662097	DQ662089	ND
Mag215_04_Mrz	PM	*M. agrestis*	M	Lung/heart	N	287	DQ768145	EF409816	ND
Mar137_04_Ebe	BAR	*M. arvalis*	M	Lung/heart	P, D	725	DQ768142	DQ768143	DQ768144
Mag551_05_Mrz	PM	*M. agrestis*	M	Lung[d]	D, N	624	DQ768147	DQ768148	DQ768149
Mag520_05_Ebe	BAR	*M. agrestis*	M	Lung/heart	N	287	DQ768146	EF409817	ND
Mag175_05_Sen	GÖ	*M. agrestis*	M	Lung	P, D, P5′, P3′	1670	EU439956	EU439949	ND
Mar121_05_Sen	GÖ	*M. arvalis*	F	Lung	P, D, P3′	1347	EU439953	EU439946	ND
Mar139_05_Sen	GÖ	*M. arvalis*	M	Lung	P, D, P3′	1347	EU439954	EU439947	EU439960
Mar174_05_Sen	GÖ	*M. arvalis*	M	Lung	P, D P5′, P3′	1666	EU439955	EU439948	ND
Mar204_05_Sen	GÖ	*M. arvalis*	M	Lung	P, D, P5′, P3′	1700	EU439957	EU439950	EU439961
Mar205_05_Sen	GÖ	*M. arvalis*	M	Lung	P, D, P5′, P3′	1708	EU439958	EU439951	EU439962
Mar222_05_Sen	GÖ	*M. arvalis*	M	Lung	P, D, P3′	1347	EU439959	EU439952	ND

[a] M, male; F, female; ND, not determined.
[b] The rodent numbers reflect the species (Mar, *M. arvalis*; Mag, *M. agrestis*), the number of the rodent, trapping year, and trapping site in the different administrative districts (for geographical localization of trapping sites, see Fig. 1).
[c] Positive reactions in the three different RT-PCRs used are indicated. D, primer pair DOBV-M6/DOBV-M8; P, PUUV 342/cPUUV 1102; N, nested primer PUUV390/cPUUV721; P3′, PUUV1104/cPUUV1758; P5′, PUU_Fpuni/PUUV c740; S1, S1/S10PC; S, SNMa1/MaS4C.
[d] The heart sample from this animal was not reactive in RT-PCR.

fered from 0.1 to 0.5% and 0 to 0.5%, respectively. The sequence divergence of these sequences from *M. arvalis* at the nucleotide and amino acid levels was slightly higher than that of Mag175_05_SEN from *M. agrestis* trapped at the same site and time, with 0.8 to 1.2% and 0.5 to 1.0%, respectively (Tables 5 and 6).

For the partial M segment, within-group calculations resulted in cluster Germany I having an average nucleotide divergence level of up to 3.5% (amino acid divergence level, 0.4%) and in cluster Germany II having an average nucleotide divergence of 4.9% (amino acid divergence, 0%), whereas in clusters Czech Republic and Poland, the average nucleotide divergences were 1.3% (amino acid divergence, 0%) and 0%, respectively (Table 5). The divergence pattern observed for the M segment sequences seems to be comparable to that found for the S segment sequences (Table 7). However, this conclusion does not take into account that different numbers of sequences were available for the various clusters.

As expected, the nucleotide and amino acid sequence divergences of S and M segment sequences from other *Microtus*-associated viruses, i.e., Yakeshi virus, Fusong virus, Vladivostok virus, PHV, ISLAV, and Khabarovsk virus, were found to be much higher.

These investigations revealed a surprisingly high level of nucleotide sequence divergence between the cluster of the novel German TULV sequences and TULV sequences from other European countries.

Comparison of the amino acid sequences of the N and G2 proteins and identification of clade-specific amino acid residue patterns. A comparison of the partial N protein spanning aa 105 to 215 or aa 121 to 215 (according to numbering in the N protein of TULV, strain Moravia, GenBank accession number Z69991) of the novel sequences revealed only three amino acid exchanges, comprising residues with identical (M188L and R213K in Mar1384_95) or similar (A208T in Mag235_03; data not shown) properties.

The observed higher level of amino acid sequence divergence between sequences from clusters Germany I and II and those from cluster Germany IV is reflected also in the amino acid sequence alignment of the N protein between aa residues 231 and 332 (numbering according to TULV reference strain NC_005227), showing the sequences from Germany IV to be much more similar to sequences from Slovakia, Czech Republic, and Croatia (Fig. 5). However, the other TULV sequences from Germany had a more unique amino acid sequence pattern than those from clusters Germany I and II. Interestingly, TULV sequences from trapping sites from the districts BAR (site EBE) and PR/

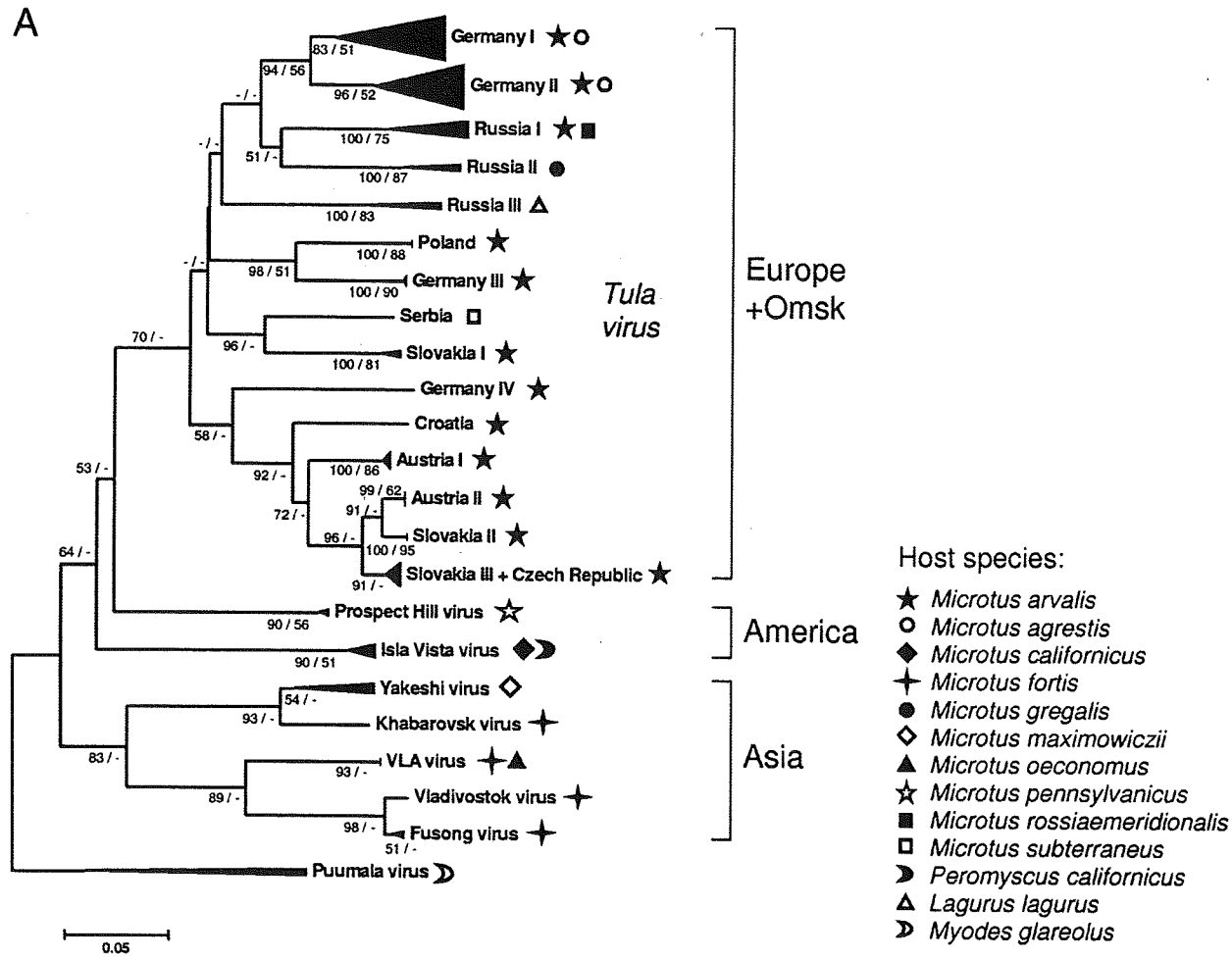

FIG. 3. (A) Phylogenetic tree (NJ tree) based on partial S segment nucleotide sequences of TULV and related viruses and information on their respective rodent hosts. Two partial S segments from PUUV (host, *Myodes glareolus*) were used as outgroups. For visibility only, clusters of phylogenetically closely related sequences were condensed to triangles (size proportional to the number of sequences) in this figure and labeled according to their geographical origin. NJ and ML algorithms were used for tree reconstruction, and the robustness of branching patterns in phylogenies was tested with 5,000 bootstrap replicates each (see Materials and Methods). Bootstrap values of >50% are given before slashes for NJ and after slashes for ML. Details of statistics for the TULV part of the phylogeny are shown in panel B. TULV records are restricted to Europe and the Omsk region in the Asian part of Russia, whereas related viruses in related rodents were detected in America and Asia. (B) The TULV part of the phylogenetic tree with the new Germany I and II clusters in detail are shown. Each cluster comprises closely related TULV lineages from both *M. arvalis* and *M. agrestis* trapped at the same locality. These phylogenetic clusters of sequences from the same locality are well supported compared to the deeper nodes connecting clusters from different regions, which is in agreement with fast evolutionary change in TULV and no recent exchange among regions. The cluster Russia I with sequences from the type locality of TULV shows the same phenomenon in the sibling species *M. arvalis* and *M. rossiaemeridionalis*, whereas the clusters Russia II and III comprise clearly distinct TULV sequences derived from different hosts caught in the same geographical region. The accession numbers of S segment sequences of TULV and other hantaviruses used for comparison are given in Table 9.

OPR (sites Granzow, Bendelin, and Nackel) had unique amino acid residues at positions 248 and 258.

A comparison of the G2 part covering aa positions 780 to 985 of the GPC (numbering in GPC of TULV, strain Moravia, according to GenBank accession number Z66538) confirmed the geographical but not host-specific clustering of TULV sequences from Germany (data not shown). Conservative amino acid exchanges were observed at position 834 with neutral V and I amino acid residues (in both *M. agrestis* and *M. arvalis* from trapping site EBE) and L residues (in both *M. agrestis* and *M. arvalis* from trapping sites MRZ and SEN) and at position 885 with neutral L amino acid residues (in both *M. arvalis* and *M. agrestis* from trapping site EBE as well as in the other five TULV sequences from Europe) and I residues (in both *M. agrestis* and *M. arvalis* from trapping sites MRZ and SEN). Interestingly, at position 834, the other five TULV sequences from Poland, Czech Republic, and Serbia had a conserved V residue. At position 976, all other European TULV strains showed a V residue, whereas the German strains had an I residue.

The amino acid sequence comparison of TULV sequences

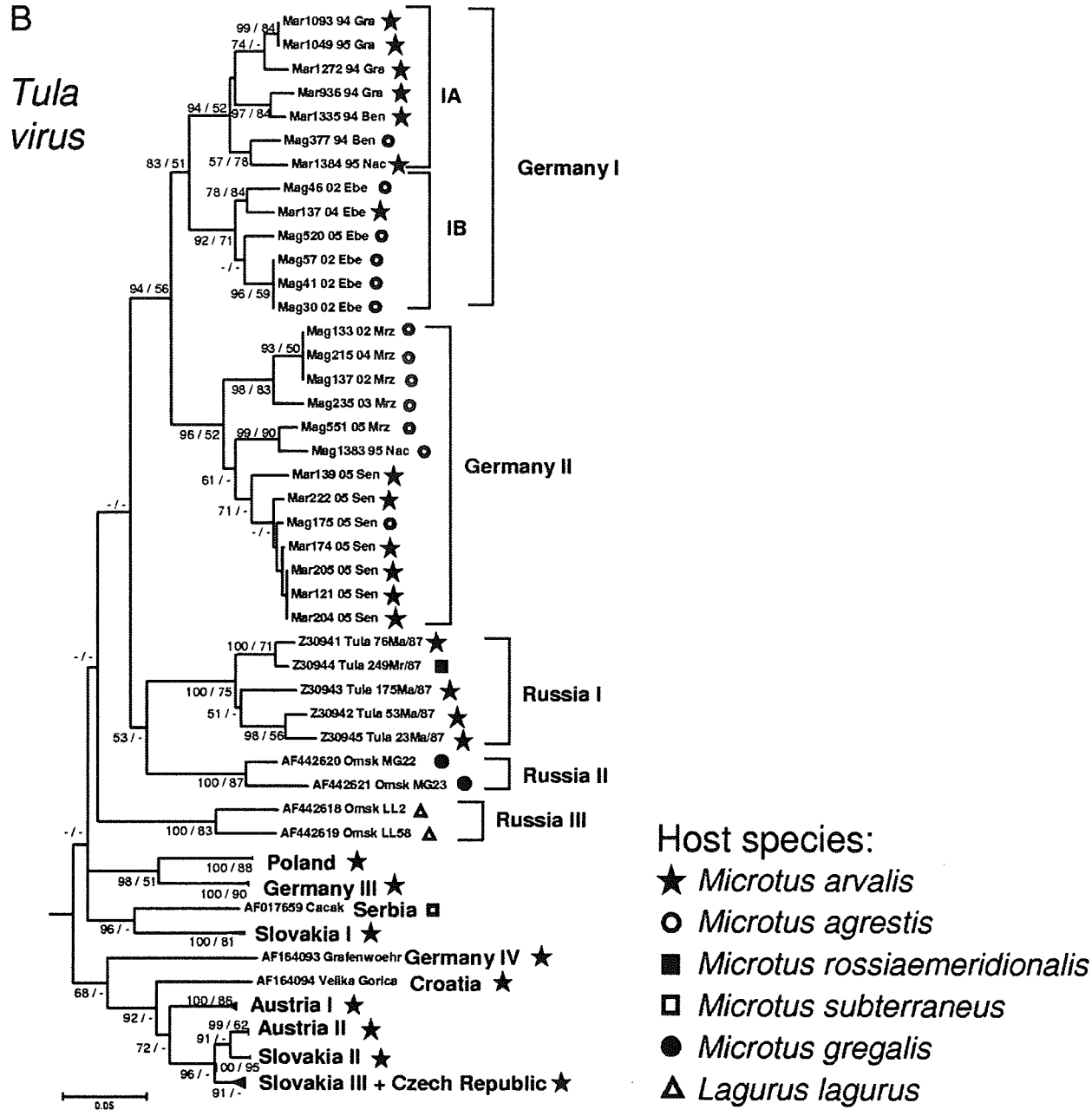

FIG. 3—*Continued.*

from certain sites resulted in the identification of trapping site-specific amino acid signatures.

DISCUSSION

In this study, we demonstrated for the first time that TULV occurs in Germany simultaneously in two different *Microtus* species, *M. arvalis* and *M. agrestis*, which is apparently uncommon for hantaviruses. However, TULV seems to be a very special hantavirus, as it has been found in a large number of different species, including *M. rossiaemeridionalis*, *M. agrestis*, *M. gregalis*, *M. subterraneus*, and *Lagurus lagurus* (43, 56, 65; Dekonenko and Yakimenko, unpublished), after its initial description in *M. arvalis* (43, 61). Similarly, other Old World hantaviruses, like Seoul virus, and various North and South American hantaviruses have been found in multiple rodent reservoir hosts (for reviews, see references 8a and 40a). These observations raise the question whether the occurrence of han-

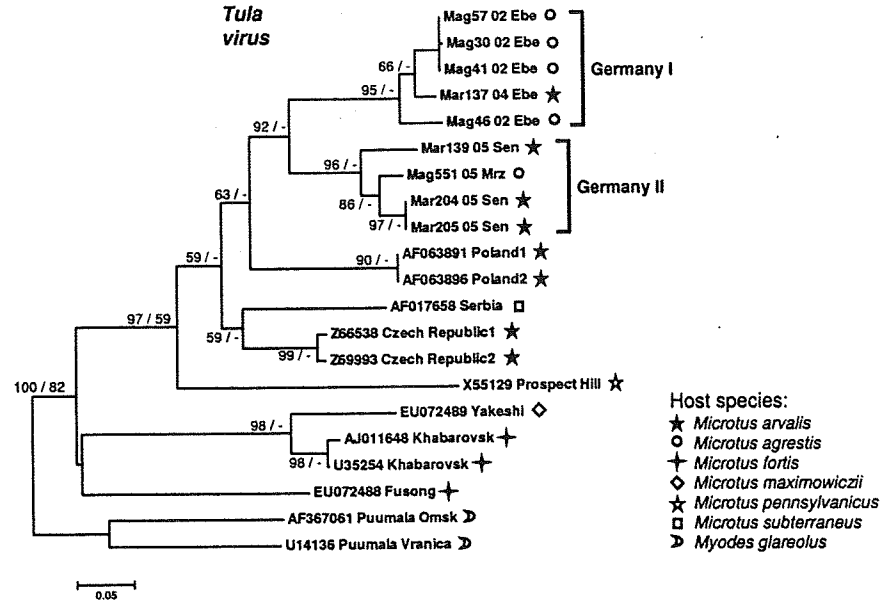

FIG. 4. NJ tree reconstructed from partial M segment nucleotide sequences of 21 TULV and related viruses. Consistent with S segment data, the new TULV sequences from Germany form two clusters according to their geographical location, independent of the respective rodent host species. The robustness of phylogenetic trees resulting from NJ and ML algorithms was tested with 5,000 bootstrap replicates each. Bootstrap values of >50% of nodes are given before slashes for NJ and after slashes for ML. The accession numbers of M segment sequences of TULV and other hantaviruses used for comparison are given in Table 10.

TABLE 5. Intercluster difference in the sequences shown in the phylogenetic trees

Cluster designation[a]	% Intercluster difference for indicated segments[b]			
	Partial S		Partial M	
	266 nt	88 aa	614 nt	206 aa
S				
Germany I (13)	7.2	0.2		
Germany II (13)	5.4	0.2		
Germany III (3)	0.3	0		
Germany IV (1)				
Russia I (5)	6.1	0.9		
Russia II (2)	5.3	2.3		
Russia III (2)	6.8	0		
Poland (2)	0	0		
Slovakia I (3)	1.9	0		
Slovakia II (4)	0	0		
Slovakia III/Czech Republic (9)	1.3	0.3		
Austria I (5)	0.3	0		
Austria II (4)	0	0		
Croatia (1)				
Serbia (1)				
Yakeshi (3)	5.0	0.6		
Fusong (2)	1.1	0.9		
VLA (3)	0	0		
Prospect Hill (2)	0.8	1.9		
Isla Vista (4)	2.2	0.1		
M				
Germany I (5)			3.5	0.4
Germany II (4)			4.9	0
Poland (2)			0	0
Czech Republic (2)			1.3	0
Serbia (1)				
Yakeshi (1)				
Fusong (1)				
Khabarovsk (2)			1.0	0.5
Prospect Hill (1)				

[a] The number of singular sequences for each cluster is shown in parentheses.
[b] Intercluster difference was measured using within-group average calculation with *P* distance models.

taviruses in different related rodent hosts might be a general phenomenon which has frequently been overlooked so far due to the lack of large-scale screenings of sympatrically occurring animals.

This paper also describes the first comprehensive study of the presence of TULV in three different regions of Germany. The initial serological detection of TULV-specific antibodies in *M. arvalis* and *M. agrestis* by ELISA using a novel homologous N antigen was confirmed by RT-PCR investigations targeting the S and M segments. RT-PCR using S segment-specific primers resulted in the detection of TULV RNA not only in lung tissue samples but also in heart and/or kidney tissue samples, which is in line with our previous observations in PUUV-infected bank voles (11). Interestingly, we were able to detect TULV-specific RNA in brain samples of seven animals from which no other tissues were available, even after storage at −20°C for 7 to 10 years. Previously, Black Creek Canal virus, a North American, *Sigmodon hispidus*-transmitted hantavirus causing hantavirus cardiopulmonary syndrome (53), was detected in rodent brain samples (24). The observed presence of TULV and Black Creek Canal virus in the brain of their natural hosts might be explained by crossing of the blood-brain barrier due to infection of newborn animals lacking an intact blood-brain barrier or of animals with pathological changes in the central nervous system microenvironment, resulting in a blood-brain barrier dysfunction. Alternatively, the presence of the virus in the brain might be mediated by infected migrating Trojan horse-like cells, such as monocytes. If crossing of the brain barrier is an outstanding property of TULV, as it is also in terms of host specificity and pathogenicity, the finding of